A MULTI-MODULAR NEUTRONICALLY COUPLED POWER GENERATION SYSTEM

A Thesis

by

VISHAL K. PATEL

Submitted to the Office of Graduate Studies of
Texas A&M University
in partial fulfillment of the requirements for the degree of

MASTER OF SCIENCE

May 2012

Major Subject: Nuclear Engineering

A MULTI-MODULAR NEUTRONICALLY COUPLED POWER GENERATION SYSTEM

A Thesis

by

VISHAL K. PATEL

Submitted to the Office of Graduate Studies of
Texas A&M University
in partial fulfillment of the requirements for the degree of

MASTER OF SCIENCE

Approved by:

Chair of Committee,	Pavel Tsvetkov
Committee Members,	Kenneth Peddicord
	Marvin Adams
	Michael Pate
Head of Department,	Yassin Hassan

May 2012

Major Subject: Nuclear Engineering

ABSTRACT

A Multi-Modular Neutronically Coupled Power Generation System. (May 2012)
Vishal K. Patel, B.S. Physics, University of Texas at Austin
Chair of Advisory Committee: Dr. Pavel Tsvetkov

The High Temperature Integrated Multi-Modular Thermal Reactor is a small modular reactor that uses an enhanced conductivity BeO-UO_2 fuel with supercritical CO_2 coolant to drive turbo-machinery in a direct Brayton cycle. The core consists of several self-contained pressurized modules, each containing fuel elements in pressurized channels surrounded by a graphite moderator, and Brayton cycle turbo-machinery. Each module is subcritical by itself, and when several modules are brought into proximity of one another, a single critical core is formed.

The multi-modular approach and use of BeO-UO_2 fuel with graphite moderator and supercritical CO_2 coolant leads to an inherently safe system capable of high efficiency operation. The pressure channel design and multi-modular approach eliminates engineering challenges associated with large pressure vessels. The subcriticality of the modules ensures inherent safety during construction, transportation, and after decommissioning.

Serpent, a continuous-energy Monte-Carlo reactor physics burnup calculation code, was used to develop a critical configuration of the subcritical modules using UO_2 fuel enriched with 5 wt% ^{235}U with a 5 wt% BeO additive. The core lifetime was found to be 14.6 years operating at 10 MW_{th}, though the U enrichment and power can be altered to achieve desired core lifetimes. Negative fuel and moderator temperature coefficients of reactivity were found that could maintain safety during operation.

The multi-modular design was found to be beneficial compared to a core with all fuel elements in one module. Batch battery type refueling was found to be beneficial and the feasibility of controlling the reactor was demonstrated through the use of control shells that surround each module.

The HT-IMMTR design is an inherently safe, highly efficient, economically competitive, and most important, feasible reactor design that takes advantage of proven technologies to facilitate the demonstration of a successful commercial deployment.

To my parents, Kaushik & Asha–the hardest working, most selfless people I know.

ACKNOWLEDGMENTS

I would like to thank my advisor, Pavel Tsvetkov for always having an open door for any issues that came up, whether personal or professional. I would like to further thank him for for sharing his expert knowledge and advice with me at every opportunity. He is a scholar and a gentleman.

I want to thank my undergraduate research advisor, Sheldon Landsberger, for taking me under his tutelage and encouraging me to pursue a career in nuclear engineering. My wonderful experience working with him is one of the main reasons I am where I am today.

Lastly, I want to thank my loved ones for always being there for me.

This material is based upon work supported under a Department of Energy Nuclear Energy University Program Graduate Fellowship.

Any opinions, findings, conclusions or recommendations expressed in this publication are those of the author(s) and do not necessarily reflect the views of the Department of Energy-Office of Nuclear Energy.

NOMENCLATURE

BOL	Beginning of life
BOP	Balance of plant
EOL	End of life
HT-IMMTR	High Temperature Integrated Multi-Modular Thermal Reactor
HTGR	High Temperature Gas Cooled Reactor
LWR	Light water reactor
LOCA	Loss of coolant accident
LOFA	Loss of flow accident
MOL	Middle of life
MW_{th}	Megawatts Thermal
SMR	Small modular reactor
wt%	Weight Percent

TABLE OF CONTENTS

Page

Page

Page

LIST OF TABLES

LIST OF FIGURES

FIGURE Page

FIGURE Page

1. INTRODUCTION

The High Temperature Integrated Multi-Module Thermal Reactor (HT-IMMTR) design concept is a small modular thermal reactor that uses an enhanced safety BeO-UO_2 fuel with supercritical CO_2 coolant coupled to turbo-machinery using a direct brayton cycle for electricity or heat generation. The core itself consists of several individual modules, each containing a subcritical fuel assembly in a graphite matrix with pressurized coolant channels attached to a power conversion system. Separately, the modules are subcritical systems, but when brought within proximity of each other, a single critical configuration is formed.

This novel approach to modularity has many benefits. The design allows for protection against criticality accidents with the use of subcritical modules that cannot become critical during manufacturing or shipping, and remain subcritical after use in the reactor. The self-consistent modules contain balance of plant machinery that can either generate electricity or produce process heat for industrial applications. Since each module self-contains the balance of plant machinery, different modules can have different balance of plant characteristics. So, in a given configuration, half the modules can be used as process heat producers and the other half can be used as electricity generators. The small uniform design of each module can allow for serial production in a domestic factory, and would not need the use of large pressure vessels typically found in large LWRs. The IMMTR is small enough to be shipped to a site by train or barge. The core is highly scalable since more modules can be added to increase core lifetime or increase the total core power.

The IMMTR design is an inherently safe, highly efficient, economically competitive, and most important, feasible reactor design that takes advantage of proven technologies to facilitate the demonstration of a successful commercial deployment.

This thesis follows the style of *Annals of Nuclear Energy*.

1.1 Small Modular Reactors

Small modular reactors are characterized by their novel design that allows for inherently safe operations for a variety of applications. An SMR is defined by the IAEA as a 300 MW_e or less reactor (IAEA, 2004). A more practical definition for an SMR is a reactor design that takes into account its small nature (small size, low power) to optimize a design for safety and performance. An example of a design features that takes the small size and low power of an SMR into account is the use of natural convection heat transfer methods. These designs can guarantee proper cooling at all times, where as a larger unit could not reliably use natural convection. A typical SMR site would consist of several SMR units such that the total output of the site can match the demand of the electricity grid.

The development of SMRs with relatively low capital costs and ability to meet a spectrum of energy needs are the ideal candidate for implementation in new and developing energy grids (Ingersoll, 2009), for use in increasing the capacity of growing energy grids, or for replacing older, less safe and less economical power plants.

Many developing countries cannot afford the large 5 billion dollar initial investment to build a large nuclear power plant. These countries are likely to build power generating facilities that are environmentally unfriendly but require less initial capital (IEA, 2009). SMRs have been shown to be economically competitive with large nuclear reactors (Carelli, 2009), but with much less initial capital–making SMRs an affordable solution to developing countries, as well as developed countries looking to expand energy generation capabilities.

Emerging grids are usually too small to allow for typical large (1000 MW_e) light water reactors, and the locations that these grids support are not economically strong enough to afford the several billion dollar capital costs for construction. SMRs mitigate this problem since if an energy grid only needed power from a single SMR, they could invest in just a one SMR, and if demand went up, the initial SMR site could easily add another unit.

1.2 HT-IMMTR Modularity

The modularity of SMRs refers to the ability to create a high power producing site with several low power reactor units (referred to as modules). In this sense, one of the biggest benefits of modularity is the ability to construct one unit, then drawing power from it to make money, while another unit is under construction. The effect of this construction style is that there is less initial capital involved, which can make nuclear power an economically viable option.

The HT-IMMTR design approaches modularity from a safety perspective. The reactor consists of several self-consistent modules. Each module is inherently sub-critical and contains all necessary equipment for proper heat removal and rejection during operation. A critical configuration is achieved when several modules come within proximity of each other. This design is inherently safe from criticality accidents during construction or shipping since a critical configuration could not be created.

Since the heat source for each module is relatively small, natural physical phenomena such as natural convection can be used as a heat transfer mechanism to guarantee safety in some accident scenarios.

The HT-IMMTR approach to modularity is also economically competitive since the modules are small and uniform in design. The construction of many modules in a serial production line facility is possible. Since many modules would be built to create one operating reactor, the learning curve associated for large construction projects would be transversed quickly such that a manufacturer could become an expert in constructing the design quickly, efficiently, and thus more economically.

During operation, the modules are directly coupled neutronically–the changes in one module directly effects the neighboring modules. This type of configuration introduces new operating challenges, especially during transient conditions. The transient analysis of this system would require a fully coupled thermal hydraulics

and neutronics analysis so the transient behavior will not be considered. However, the neutronics of a LOCA will be considered.

The ability to shuffle or replace modules mid-cycle, the effects of a single module accident, and the benefits and disadvantages of a multi-modular design versus a single module design are all investigated. This study only takes into account the neutronic physics of the reactor so it will not be able to completely account for exact operating conditions, but many aspects of operational behavior can be learned from the neutronics analysis.

1.3 High Temperature CO_2 Cooled Reactors

Advanced gas-cooled reactors are passively safe, thermodynamically efficient, and proliferation resistant reactors that can be used for electricity generation or high temperature heat production for industrial applications such as water purification or hydrogen production. With over 52 CO_2 gas cooled reactors and critical assemblies, CO_2 gas cooled reactors are a proven technology with operating history in the form of Magnox and AGR designs (Shropshire, 2004).

High temperature gas cooled reactors are the Generation IV reactor successors of the gas cooled reactor. HTGRs have features such as inherent safety characteristics, high operating temperatures, and high burnup fuel. Inherent safety comes from having a large amount of graphite in the core to act as a large heat sink if normal cooling capabilities are not available. A negative fuel reactivity temperature coefficient along with coolants that do not interact much, or at all neutronically also increase the safety of HTGRs. High operating conditions are available through the use of high temperature materials and gas coolants that are able to withstand harsh operating environments. TRISO fuel is used for its ability to withstand high temperatures and contain fission products through a strong physical barrier. The HT-IMMTR has all of these features except for the TRISO fuel; opting for a BeO-UO_2 enhanced conductivity fuel (McDeavitt et al., 2010).

The supercritical CO_2 brayton cycle is being actively researched and shows a high potential for use in reactor operations. The properties of CO_2 vary rapidly near the critical point, such that the control of a power generation system operating near these conditions is difficult. The use of supercritical CO_2 for controllable power generation has been shown to be feasible (Wright et al., 2010). Several operating configurations for the $ScCO_2$ cycle have been previously studied (Dostal, 2004) and have been shown to achieve theoretical efficiencies upwards of 45%. In comparison, LWR water rankine cycles have efficiencies of about 33%, meaning the $ScCO_2$ brayton cycle could be much more economical than an LWR rankine cycle.

1.4 Design Objectives

The system is intended for use either autonomously or with operator control depending on intended application. The modular nature of the reactor allows for power production in rural environments and/or heat production in industrial applications (concurrent operation is possible).

The modules are expected to operate in a battery type configuration, e.g., be shipped to a site, operated for several years, and then shipped back to a post-processing facility. This configuration has the potential to have batch fuel reloading during operations by switching out whole modules.

The BeO-UO_2 (LEU) fuel is an enhanced thermal conductivity concept fuel that facilitates reactor operations and increases safety of operation. The enrichment of BeO and ^{235}U in the fuel will be investigated. For economic and proliferation concerns, the fuel enrichment is to be minimized with respect to reactor performance characteristics.

Two materials are investigated for use in the reactor, Zr and stainless-steel 304. The optimal fuel pin pitch to diameter ratio will be found and the fuel enrichments and number of modules will be varied to find an optimal operating configuration.

A core lifetime greater than 5 years at a total power level of 10 MW_{th} is envisioned. Higher core power levels are expected to be possible, and the addition of more modules can increase the total core power level or increase the core longevity, depending on what is desired.

The BOP side of the reactor will not be analyzed, but factors such as core power distributions and reactivity coefficients that are integral to a thermal hydraulics analysis will be found.

1.5 Thesis Objectives

The objective of this thesis is to establish a viable HT-IMMTR design and to evaluate the modular design for performance and safety.

The design parameters to evaluate are:

- Fuel pin characteristics:
  - ^{235}U and BeO Enrichment
  - Pin location
- Reactor vessel and cladding materials:
  - Stainless Steel 304
  - Zirconium
- Module characteristics:
  - Geometry configuration and placement
  - Total number needed for operation

The performance of the core will be measured by:

- Core Lifetime
- Power level

- Response to operating conditions unique to the novel modular design
  - Battery type refueling
  - Module reshuffling
- Differences between one large module and a multi-module configuration

The safety will be analyzed by considering:

- Temperature perturbations
- LOCA event
- Power shape and peaking
- Point reactor kinetics parameters
- Modular accident events
  - Single module LOCA
  - Single module removal
- Control rod placement

2. APPLIED CODE SYSTEMS

This analysis was driven by Serpent, which is a tool that uses the Monte Carlo method to simulate reactor physics. This tool was supplemented by Python 3, Microsoft Excel and Simulink Matlab for input preparation, and output post-processing.

2.1 Serpent

The reactor neutronics were modeled in Serpent (version 1.1.16). Serpent (Leppänen, 2011) is a continuous-energy Monte Carlo reactor physics burnup calculation code. Serpent is capable of full core reactor physics and burnup calculations. It can model almost any two or three dimensional reactor design by using a universe-based geometry model. Serpent was used to solve for core multiplication factors, burnup, and flux and power distributions on a uniform cartesian mesh. The main advantage of Serpent over other Monte Carlo methods is its speed.

The speed of Serpent is attributed to the code pre-calculating reaction cross sections on a single unionized energy grid before transport begins. This means when a reaction occurs at a certain energy, the relevant data can just be looked up from a table rather than calculated on the fly. This leads to the code using a large amount of RAM rather wastefully, but it speeds up calculation times substantially. Another reason for the speed is that Serpent uses the Woodcock delta-tracking method (Leppänen, 2010) to track neutrons. This particle tracking method is advantageous because it does not have to compute distances to boundaries during the random walk analysis. Instead a total core homogenized cross section is generated and a sample rejection process is carried out at each possible interaction event. In complex geometries, this method is much less computationally taxing than MCNP's surface tracking method in which distances from the particle to boundary surfaces must be computed.

A drawback of this method is that since it does not consider surface boundaries, track-length estimators for flux integrals are not available, instead collision estimators are used. Also the efficiency of the method degrades near highly absorbing materials. When the efficiency of the calculation is low, Serpent switches to a traditional surface tracking method. The main concern for using Serpent is that it is not a well benchmarked code like MCNP is and thus final results must be verified in using MCNP or similar, recognized tools.

2.1.1 Code-to-Code Verification with MCNP5 & MCNPX

Serpent is a new code system and as such is not as widely used or widely verified and validated as the Monte Carlo N-Particle (MCNP) code. MCNP5 (X-5 Monte Carlo Team, 2008) is a general purpose neutron, photon, and electron transport code for nuclear criticality safety, and health physics applications and MCNPX (Pelowitz, D (Ed.), 2008) allows for burnup calculations. To test if Serpent is a valid tool to use for reactor physics calculations of the HT-IMMTR, the same geometry was created in Serpent and MCNP, and results were compared. Positive results are not indicative of the codes providing correct answers (validation), it just indicates that the two codes solve a problem and get the same answer (verification).

Thermal Scattering Data

Thermal scattering laws are used to take into account the crystalline and molecular structure effects of compounds on scattering cross sections in the thermal range that could not be accurately modeled with a free gas model. Serpent does not natively have thermal scattering law data for UO_2 fuel, so this data was imported from MCNP. The inclusion of scattering data was thought to increase the accuracy of the results but also increase computer time. Serpent was ran with the thermal scattering data and without the data, and the results are compared with MCNP in

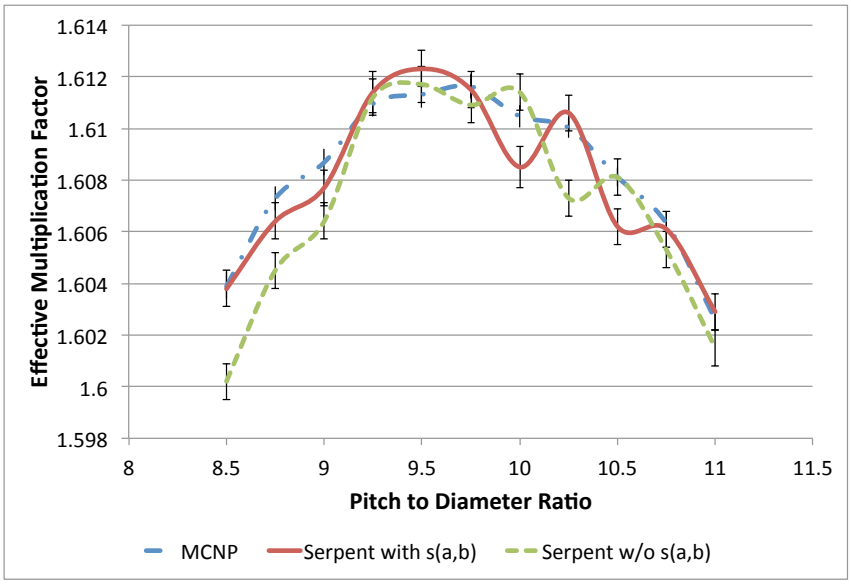

Fig. 2.1. MCNP vs Serpent Infinite Fuel Lattice Case with 5% ^{235}U Zr Cladding Case.

Fig. 2.1. The run time of the calculations with thermal scattering data for the fuel was found to be only a few percent more than the no fuel thermal scattering law case. The serpent model with thermal scattering data agrees within uncertainty to the MCNP results, whereas without the scattering law data, the data do not agree. It is therefore important to include the thermal scattering data for the fuel.

Flux Comparison

The neutron energy spectrum shows the energy dependent neutron flux. The spectra generated in MCNP and Serpent are shown in Fig. 2.2. The fluxes predicted in both cases agree with each other within uncertainty. The flux was computed using 100 energy bins equally spaced in lethargy space. The two codes are normalized to a specific power using different techniques. MCNP output tallies carry the "unit"

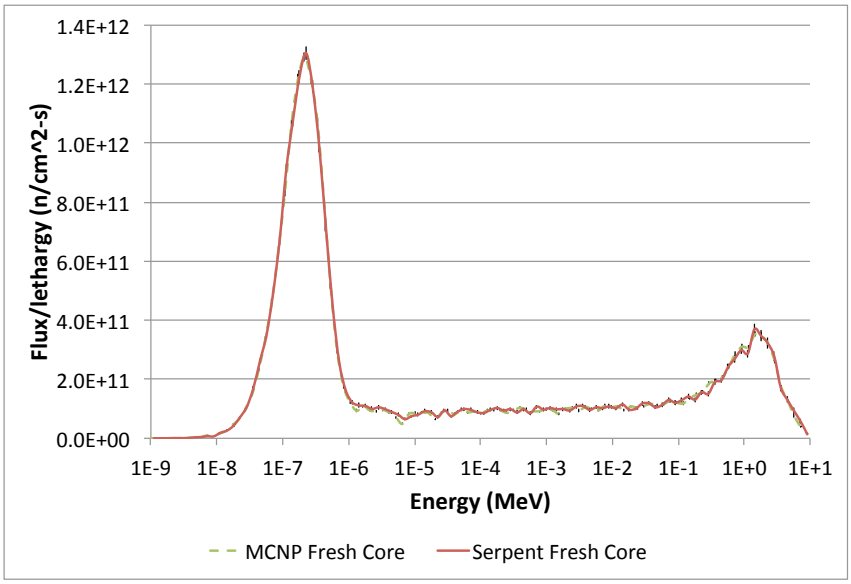

Fig. 2.2. MCNP vs SERPENT Flux in Inner-Most Fuel Pin.

per unit starting particle, so to adjust the tally to a certain power level, each tally should be multiplied by

$$C_0^{MCNP} = \frac{P_0 \bar{\nu}}{E_f \mathrm{k_{eff}}}, \tag{2.1}$$

where P_0 is the operating power level, $\bar{\nu}$ is the number of neutrons produced per fission, E_f is the energy per fission, and $\mathrm{k_{eff}}$ is the effective multiplication factor. Serpent output tallies carry the "unit" per unit loss rate and are calculated assuming a volume of unity. To adjust the output to a power level, each tally should be multiplied by

$$C_0^{Serp} = \frac{P_0}{P_{\mathrm{abs}} V}, \tag{2.2}$$

where C_0^{Serp} is the normalization constant, P_0 is the operating power level, P_{abs} is the power level given in the Serpent results file, and V is the volume of the region that is being tallied. Alternatively, properly normalized tallies can also be outputted by Serpent using the "set power" command while specifying the volume on the detector input (though volumes cannot always be calculated accurately by Serpent).

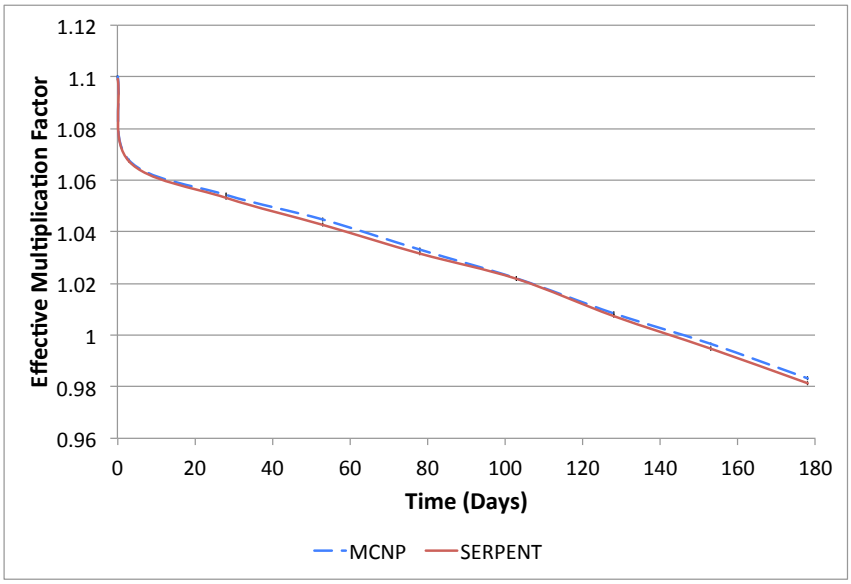

Fig. 2.3. Core Lifetime Predictions Comparison for a 100 MW HT-IMMTR.

Burnup Comparison

A key figure of merit in a reactor analysis is the expected core lifetime. Comparative results from a 178 day burnup cycle with 8 burn steps at 100 MW of the HT-IMMTR are shown in Fig. 2.3. Both codes predict a core lifetime of about 128 days and are within error of each other at each burnup step. In general, the statistical error associated with burnup calculations is much less than the actual error, and the quoted lifetime should have an implicit error of about 15%.

2.1.2 Shannon Entropy

To get reliable results from Monte-Carlo calculations, some initial cycles need to be skipped such that k_{eff} tallies are taken only when the neutron population is in the fundamental mode. This is typically achieved once k_{eff} does not change appreciably between cycles. Another test that needs to be passed to ensure reliable results for any other tally, such as a flux tally, is that the shannon entropy (Ueki and Brown,

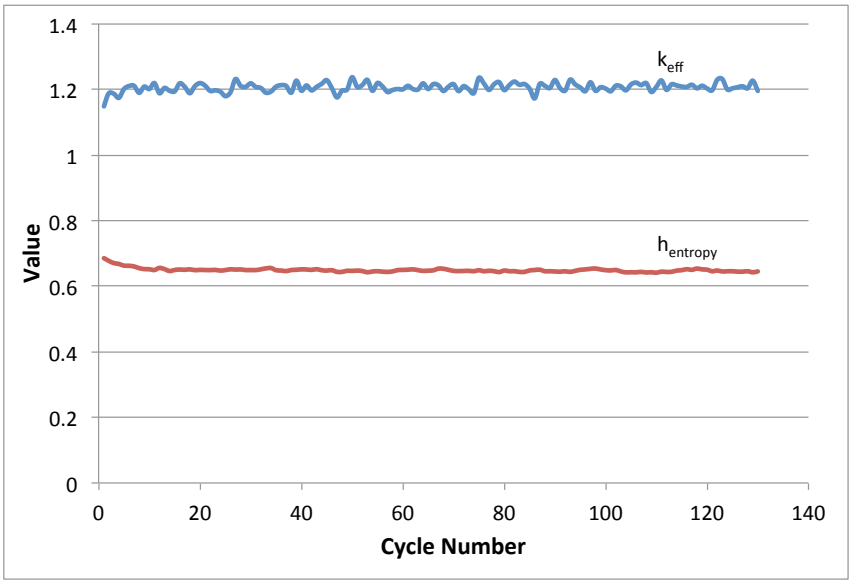

Fig. 2.4. Shannon Entropy and k_{eff} Dependence on Cycle Number.

2002) should not change appreciable between cycles. The shannon entropy and the k_{eff} of the reactor is shown in Fig. 2.4. At least 20 cycles should be skipped when doing Serpent calculations on the HT-IMMTR.

2.2 Computer and Code Systems

The main computer with which this work was completed on was a 3.4 Ghz Intel Core i7 iMac with 12 GB of ram running Mac OS X Version 10.7. The TAMU Nuclear Engineering Grove cluster was used as a secondary machine when the primary was unavailable. The Grove cluster consists of 20 Intel Xeon 5345 Quad-Core processors with 4 GB of ram per processor running RedHat Enterprise Linux WS 4.

Along with Serpent, Python 3 was used to create Serpent input files and post-process Serpent output files. A script was made that determined geometry locations based on user inputed geometry dimensions. These locations were used to create Serpent input files. Burnup output files were parsed for nuclide inventory vectors

over time such that new Serpent input files could be made utilizing these vectors for anytime during the reactor lifetime. Large detector (or tally) outputs that could not efficiently be handled by Matlab were broken up into smaller, more manageable files that Matlab could read.

Matlab (MATLAB, 2010) was used to visualize the reactor flux and compute various quantities of interest from Serpent output files. Excel was used when data had to be compared visually such as reactor lifetime plots.

This document was generated by the LaTeX document typesetting system.

2.3 Parameters

Serpent requires many input parameters that are set by the user. The value of these user inputs generally directly effect the accuracy and precision of the codes output.

The most important input is the choice of the nuclear data library since different data libraries will give slightly different results. The nuclear data library contains all the point-wise neutron cross sections that are used in the transport calculation. The ENDF/B-VII nuclear data library was used in this analysis.

The number of particles to run, along with the number of cycles to skip and to tally are also important. Too few particles will result in large statistical errors, and too many particles will result in very long runtimes. A balance between good statistics and reasonable runtimes must be used. For criticality calculations, 10000 particles were used with 30 cycles skipped and 100 cycles tallied. To resolve quantities such as the flux of the core, more particles are needed because the flux is usually tallied on a small region of the reactor such that the number of neutron interactions in the small region is low, leading to poor statistics of results. For full core power distributions, 10000 particles were used, skipping 30 cycles and logging 1000-3000 cycles, depending on the specific run.

The core power and flux distributions were found by tallying the relevant reaction rate in fuel area of the reactor on a 300x300x40 voxel cartesian mesh. This mesh was large enough to cover the whole fuel and outer reflector area. The mesh was also fine enough to resolve pin power rates. Other distributions were found using specific geometry as reference points, such as the neutron energy flux in the center most fuel pin.

The burnup simulations were conducted using 10000 particles per cycle, with 30 skipped cycles and 100 logged cycles. The number of burn-steps was varied in each problem depending on the total burn time. Each burn-step was 90 days long, except for the first three which were at 0, 3, and 25 days. These initial steps are close together to take into account Xenon production.

3. REACTOR CONCEPT

The HT-IMMTR is an SMR design that consists of several subcritical modules that are arranged in a single critical core configuration. Each module is self consistent in that it contains all the machinery needed for safe operations, except for the critical geometry. This configuration eliminates criticality accidents during construction and shipping, as well as allows for electricity generation or heat production concurrently since each module can have different BOP machinery.

The full core model of the reactor is shown in Fig. 3.1. Each modules contains LEU BeO-UO_2 fuel in pressure channels in a hexagonal graphite matrix. The fuel is cooled by $ScCO_2$ that is used in a direct Brayton cycle. The $ScCO_2$ flows from the bottom of the core, through the pressure channels, into the upper plenum and turbo-machinery, through the downcomers and back into the bottom of the core. Several modules are placed into a graphite matrix to form a critical geometry.

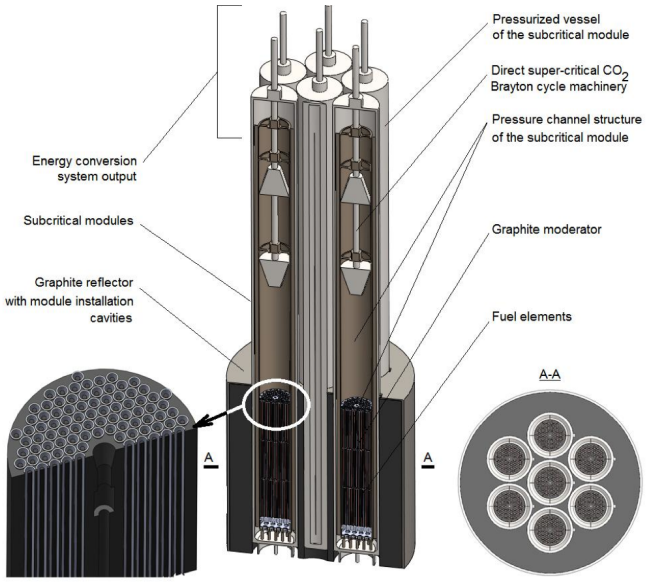

Fig. 3.1. Full Core View of HT-IMMTR Concept.

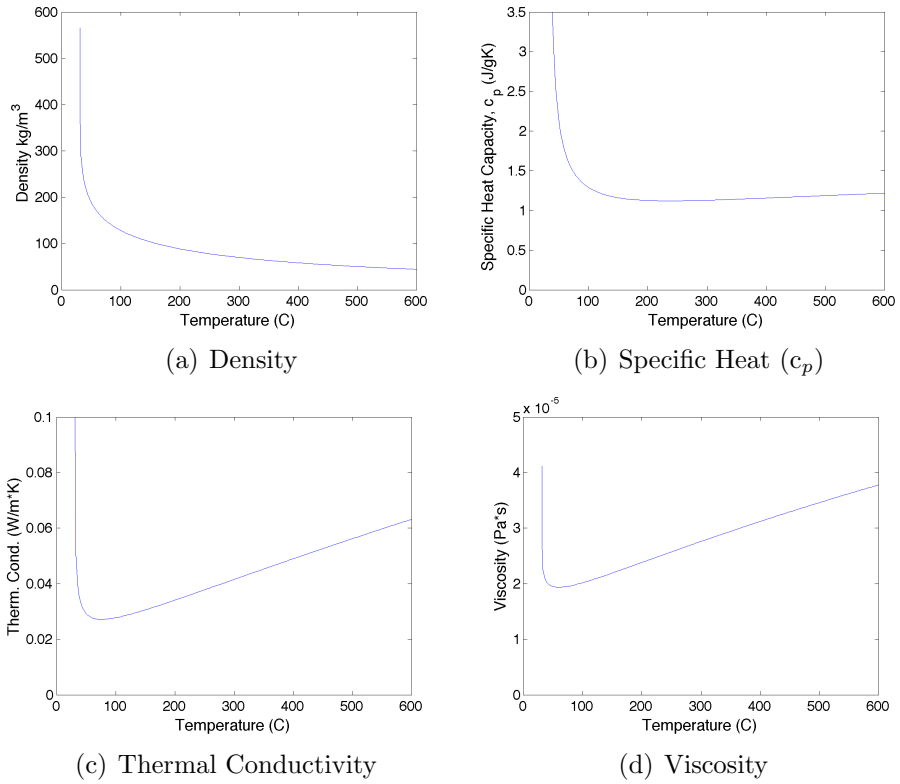

(a) Density (b) Specific Heat (c_p)

(c) Thermal Conductivity (d) Viscosity

Fig. 3.2. Variations of Thermodynamic Properties of Supercritical CO_2 with Temperature (7.4 MPa).

3.1 Supercritical CO_2 Coolant

Supercritical CO_2 is used as the working fluid in a direct Brayton cycle for the HT-IMMTR. Relatively high efficiencies (above 45%) have been shown (Gibbs, 2008) for working pressures of 20 MPa and outlet temperature of 650 °C.

The thermodynamic properties of supercritical CO_2 depend highly on pressure and temperature (see Fig. 3.2). The thermal properties of the fluid change very rapidly near the critical point (see Fig. 3.3). The non-linearly varying properties of CO_2 near the critical point bring in stability and operations concerns (Dostal, 2004), however an operating system was created (Wright et al., 2010) to show that it is possible to operate safely near the critical point.

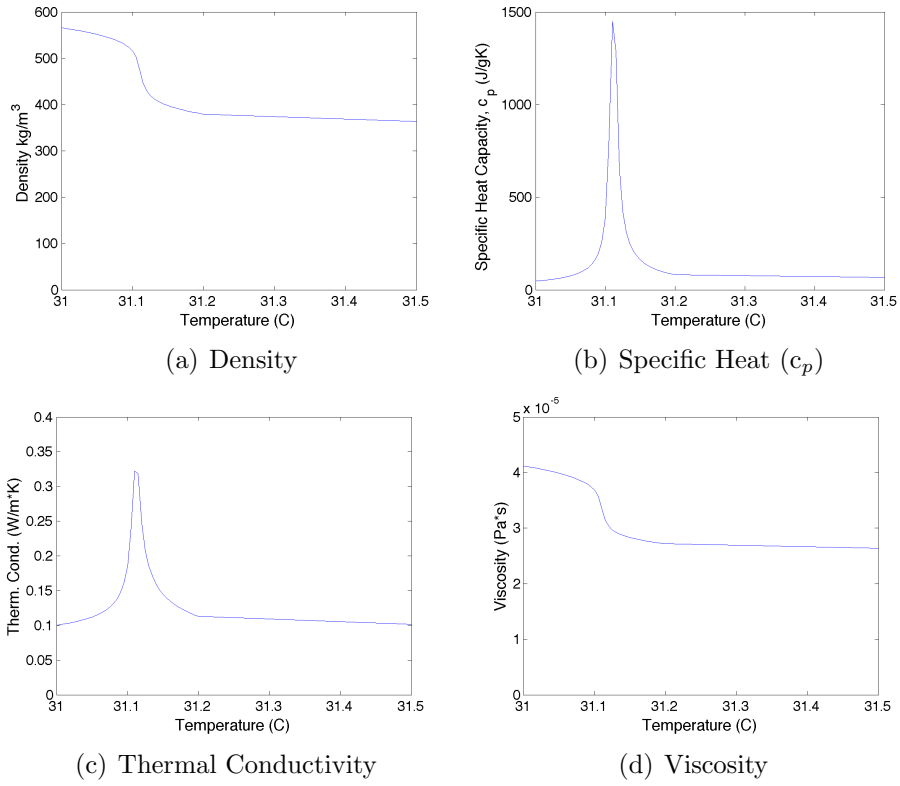

(a) Density (b) Specific Heat (c_p)

(c) Thermal Conductivity (d) Viscosity

Fig. 3.3. Variations of Thermodynamic Properties of Supercritical CO_2 Near the Critical Point (7.4 MPa).

The use of $ScCO_2$ in a direct Brayton cycle allows for high efficiency operations. Operating the heat rejection portion of the cycle near the critical point (7.38 MPa, 31 °C) allows for efficient heat rejection; there is a large peak in the heat capacity at this state, so heat is essentially transferred isothermally. The compressor inlet condition of the $ScCO_2$ should be near the critical point, which allows for low power compression work compared to non supercritical CO_2 since the density of the $ScCO_2$ fluid is large. Low power compression allows for less work to be lost to operating the cycle, and thus allows for more total useful work, increasing the cycle efficiency.

An advantage of $ScCO_2$ is that it can interact with fission products and deposit them on surfaces in the reactor. The deposition process can potentially be controlled

such that fission products that escape the fuel are deposited in specific areas, which can then be analyzed to determine the integrity of fuel during operation.

$ScCO_2$ does interact with the neutronics of the system and depending on the system configuration, can cause a positive or negative reactivity insertion in a LOCA. The effects of a LOCA on reactivity will be investigated.

3.2 Fuel and Pressure Channel Design

A BeO-UO_2 enhanced conductivity fuel is used in the reactor design. The fuel, in pellet form, is placed into long cylindrical pins. The fuel pin is surrounded by a cladding material that is to be determined. The clad is in contact with the $ScCO_2$ coolant, which is all enclosed in a pressure channel that is surrounded by graphite. The fuel geometry is shown in Fig. 3.4.

The BeO in the fuel has been shown (Andrade et al., 2007) to more than double the thermal conductivity of UO_2. An increase in thermal conductivity means the fuel centerline temperature will be lower than a fuel with low thermal conductivity. This allows for safer operations since the fuel can operate with higher safety margins. One drawback is that the BeO-UO_2 compound has a eutectic point of 2160 °C, which is small compared to UO_2's 2865 °C melting point. This means in transient conditions, the fuel may be more prone to melting.

The economics of BeO-UO_2 fuel are tricky since there is no fuel cycle operating with this fuel. The cost of the BeO-UO_2 fuel cycle depends greatly on the Be content of the fuel and the fuel cycle length. It has been shown (Kim et al., 2010) that the economics of this fuel cycle gets more viable with increased fuel burnup.

The use of $ScCO_2$ and graphite in the same design can lead to a CO_2-graphite oxidation reaction which can change the thermodynamic properties of graphite, as well as degrade the graphite geometry. To remove the possibility of such interactions, the fuel and coolant are placed in a pressure channel that is a physical barrier between the graphite and the coolant.

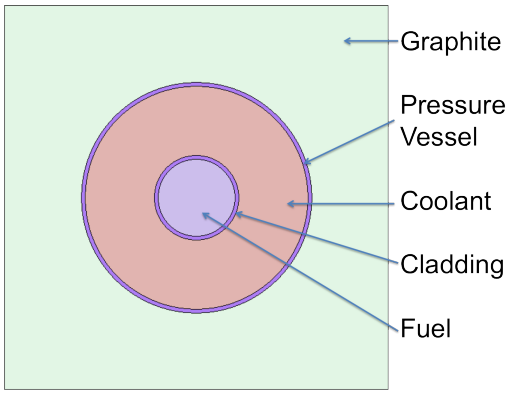

Fig. 3.4. Fuel Pin Geometry.

3.3 Cladding and Pressure Vessel Material

The pressure vessel and cladding material are design options that must be investigated. The two choices that will be investigated are Zr and stainless steel 304. There are two pressure vessels in each module, and outer and inner.

The inner pressure vessel creates pressure channels in the fuel area and an upper plenum for the BOP machinery. The outer pressure vessel surrounds the inner pressure vessel and creates flow areas for the $ScCO_2$ to come from the upper plenum into the lower plenum and back into the active fuel area.

The cladding surrounds the fuel, and gives it structural support as well as acts as a physical barrier for fission products.

The ideal material for the pressure vessel and cladding is a material that is structurally stable in a high temperature and high radiation environment, neutronically transparent, and economical. No such material exists so compromises must be made.

3.3.1 Stainless Steel 304

Austenitic stainless steels are used in many nuclear reactors as structural materials and as cladding materials in AGR systems. It is able to handle a large neutron fluence, so it's a prime candidate for use in a nuclear reactor (Chopra et al., 2006).

Stainless steel is a good reflector of fast neutrons, but it absorbs thermal neutrons. Since the leakage of neutrons out of each module is important for criticality of the HT-IMMTR, the neutron absorption properties of SS may be a large problem.

3.3.2 Zirconium

Zirconium in the form of a nuclear grade zircaloy-4, which is typically greater than 95% Zr with almost no Hf, has been used as a cladding material in many LWRs. Its use in reactor operations has been proven and thus is a great candidate for a new nuclear reactor design.

Zircaloy however is expensive at 55,000 $/tonne (Burnham et al., 1970) versus 3222 $/tonne stainless steel 304 (MEPS Online Steel Prices, 2012). Though this is a huge cost difference, the presence of SS in the core will require a larger fuel enrichment, which also costs a lot and can offset the materials price.

Zirconium has a low neutron capture rate, and is able to withstand high temperatures and radiation environments. One drawback of Zr for use in LWRs is the Zr-H_2O interaction that can create hydrogen gas that degrades the performance of the reactor. Since there is no water in the HT-IMMTR design, this drawback is eliminated.

Zircaloy-4 undergoes a phase transition at about 900 °C (Terai et al., 1997), so in the high temperature environment of the HT-IMMTR, it is not the best material to use. However, since this study is on the neutronics of the core, this material will still be considered. A different high temperature cladding would be needed to actually create this reactor.

3.3.3 Alternative Materials

Not many materials exist that can survive in the high temperature, high radiation environment inside a nuclear reactor. Silicon Carbine (SiC) has been used in TRISO fuels since SiC acts as a diffusion barrier to fission produces. However, the carbon in SiC has the possibility of interacting with the $ScCO_2$ in the same way graphite would interact, so it is not a good material to use in the HT-IMMTR.

Magnesium non-oxidizing, or Magnox was used as cladding in the CO_2 cooled Magnox reactors. It would be a prime candidate except that it has a relatively low melting temperature such that a Magnox clad would melt if used in the HT-IMMTR.

3.4 Module Applications

The HT-IMMTR design is deliberately small, and not just a scaled down version of a larger reactor. This allows for many unique features that are not possible with large power reactors.

The HT-IMMTR can be built in rural environments and has the potential for autonomous operation. The ability for the reactor to be built in a factory and then shipped to a site allows for the HT-IMMTR to be able to operate anywhere that it can be shipped to. The simple design means reactor control operations can be handled by a computer, or at the very least only a small staff would be required.

The small reactor size allows for phenomena such as natural convection to be a potential heat removal method after a reactor SCRAM. The lower power output of the small design causes the amount of radionuclides in the reactor, called the source term, to be reduced relative to a larger plant. This allows for a safer design since when comparing the reactor to a larger reactor in the worst case scenario (a release of radionuclides), the HT-IMMTR would release much less radionuclides to the environment.

The reactor is specifically targeted to be grid size appropriate. New and growing energy grids are typically not large enough to accommodate large 1000 MW nuclear reactors. They therefore have to rely on other non-sustainable or inefficient energy sources. Energy grids with many small plants allows for a more stable grid and the construction of smaller plants has been the trend in the last decade (Ingersoll, 2009).

The modular nature of the HT-IMMTR allows for concurrent electricity and heat production. Since each module contains its own BOP equipment, some modules can be fitted with electricity generators and others with process heat equipment. Also, because the BOP area is separate from the fuel area within each module, the two sides can be built separately and then combined. A simple block diagram of the BOP layout for a module that produces electricity is shown in Fig. 3.5

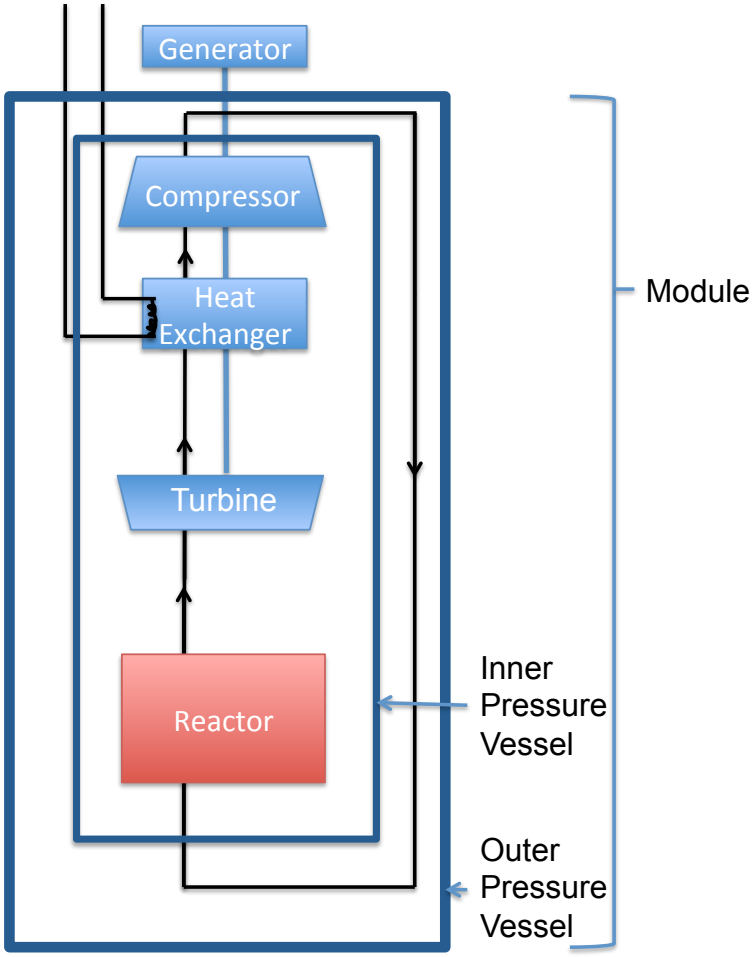

Fig. 3.5. BOP Configuration for an Electricity Producing Module.

4. DESIGN ANALYSIS

The concept of the reactor design has been developed. The specific properties of the reactor now need to be analyzed. There are several design choices that can be made from a neutronics analysis. The optimal geometry for the largest possible k_{eff} will be found, the better core cladding and pressure vessel material between Zr and SS will be found from a comparative study, the fuel enrichment and BeO concentration will be chosen, and the size of the core will be found.

The size of the reactor will be partially optimized by finding the optimized outer reflector radius. To optimize other geometry dimensions, such as the downcomer radius, upper and lower plenum heights, and the coolant channel radius, a thermal hydraulics study would need to be conducted.

The core power and flux distribution will be determined. The distributions can be used in a safety analysis and will be used to determine locations for control rods.

4.1 Fuel Enrichment, Cladding and Pressure Vessel Material Choice

A 20 wt% BeO, 80 wt% UO_2 fuel is used to achieve conservative values. The BeO wt% will be optimized after deciding the fuel enrichment and cladding material. Three fuel enrichments of 5%, 10%, and 15% enriched ^{235}U are considered along with two choices of cladding: stainless-steel-304 or Zr, for a total of 6 test cases.

4.1.1 Optimal Lattice Pitch to Diameter Ratio

There exists an optimal geometry for a given thermal reactor configuration. This arises from the relationship between the amount of fuel and the amount of moderation in the core, commonly referred to as the fuel to moderator ratio. The geometry will first be optimized at the infinite level. To find the optimal fuel pin locations in the

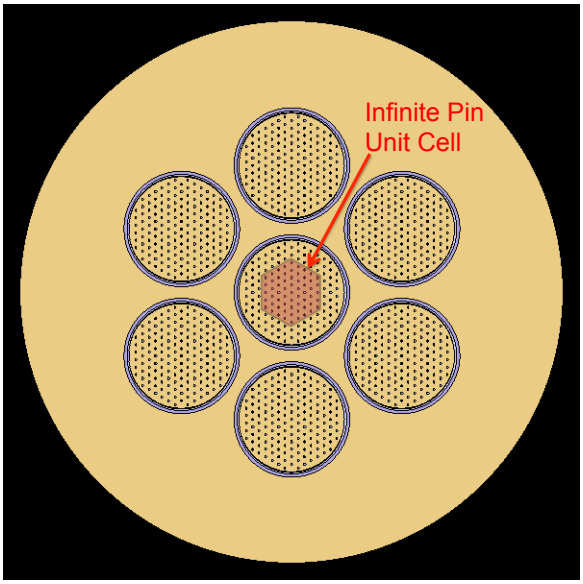

Fig. 4.1. Infinite Pin Cell Lattice Modeled in Serpent.

core, k_∞ should be plotted against the fuel to moderator ratio. The fuel to moderator ratio that produces the maximum k_∞, is the optimal geometry.

A method of changing the fuel to moderator ratio is to change the pitch of the pin, leaving the pin diameter constant. Plotting k_∞ against the pitch to diameter ratio will give the optimal infinite geometry.

An infinitely tall fuel pin located in an hexagonal graphite element was modeled in Serpent. Reflective boundary conditions were imposed on the boundaries of the hexagonal element to create an infinite fuel lattice. The modeled area can be seen in Fig. 4.1, where the actual geometry would be the shaded hexagonal region repeated infinitely. The 20% BeO 80% UO_2 fuel is surrounded by cladding that is either SS-304 or Zr. The cladding is surrounded by a CO_2 coolant channel, which is surrounded by more cladding material. The outer cladding material ensures that the supercritical CO_2 cannot interact with the graphite moderator.

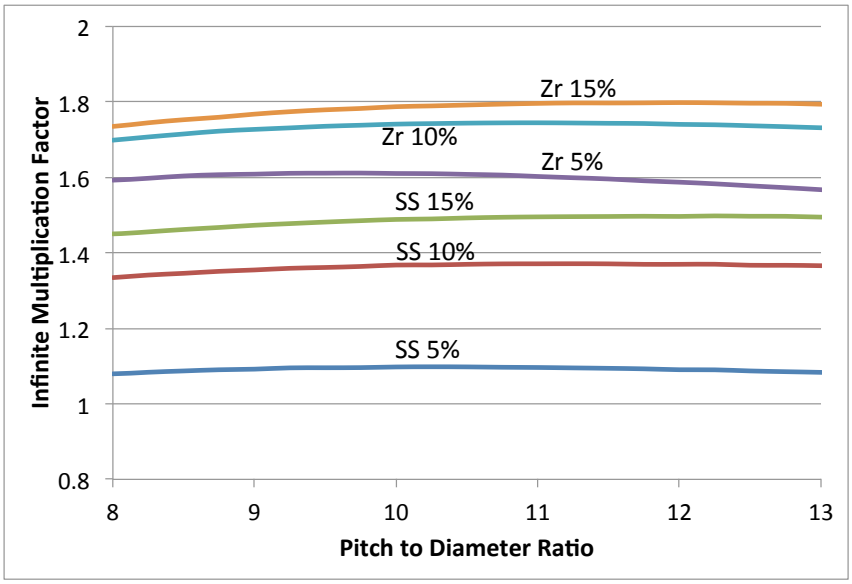

Fig. 4.2. k_∞ Dependence on Infinite Fuel Pin Lattice Pitch to Diameter Ratios for Various ^{235}U Enrichments and Cladding Materials.

The active fuel radius was .5 cm with a 1 cm thick clad; both kept constant. The pitch to diameter ratio is defined to be

$$PD_{fuel} = \frac{\text{Pitch}}{\text{Diameter}} = \frac{\text{Distance Between Adjacent Fuel Pin Centers}}{\text{Active Fuel Diameter}} \tag{4.1}$$

where PD_{fuel} is the pitch to diameter ratio of the infinite fuel pin lattice. The pitch was changed by changing the width of the infinite hexagonal matrix. The fuel pitch was varied and the multiplication factor of the different configurations were found and the results are shown in Fig. 4.2.

All 6 test cases resulted in a super-critical system with all of the Zr cases having more reactivity than the SS-304 cases. This is because SS-304 has a larger neutron absorption cross-section than Zr. Although the SS-304 cases had a lower multiplication factor than the Zr cases, the design will be carried forward to see differences at the module level. The optimal pitch to diameter ratios are shown in Table 4.1.

Table 4.1
Optimal Pitch to Diameter Ratios for Various Fuel Enrichments and Cladding Types.

Enrichment	Cladding	PD_{fuel}	k_∞
5%	SS-304	10.25	1.09834 ± 0.00047
10%		11.25	1.37139 ± 0.00047
15%		12.25	1.49809 ± 0.00047
5%	Zr	9.75	1.61162 ± 0.00046
10%		11	1.74482 ± 0.00050
15%		12	1.79833 ± 0.00046

4.1.2 Optimal Module Pitch to Diameter Ratio

The actual fuel elements are located within a module, and the modules have a pitch between one another. The module pitch to diameter ratios is

$$PD_{\text{mod}} = \frac{\text{Distance Between Module Centers}}{\text{Diameter of the Module}}. \tag{4.2}$$

Since the fuel lattice was optimized at the infinite level, deviations from this configuration should reduce k_∞, since the changes made are poisonous to the neutron economy. The optimal PD_{mod} would be 1, but that introduces engineering difficulties, so a $PD_{\text{mod}} > 1$ is preferred. The effect of the PD_{mod} on k_∞ needs to be found.

An infinitely tall fuel module located in an hexagonal graphite element was modeled with reflective boundary conditions on the boundaries of the hexagonal element to create an infinite fuel lattice. The modeled area can be seen in Fig. 4.3, where the actual geometry would be the shaded hexagonal region repeated infinitely. The fuel pins are surrounded by a 1 cm thick inner pressure vessel, a 1cm thick CO_2 down-comer, and a 4 cm thick outer pressure vessel.

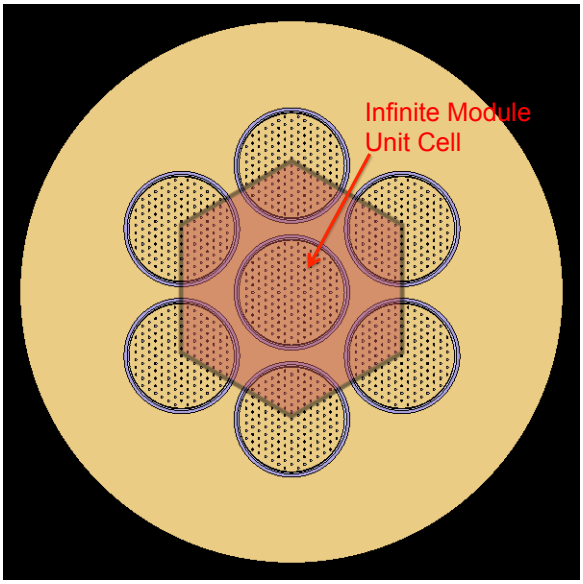

Fig. 4.3. Infinite Module Lattice Modeled in Serpent.

The module pitch to diameter ratio was varied by changing the distance between the centers, leaving the module diameter constant. The results in Fig. 4.4 show the Zr cases are super-critical, whereas only the 15% enriched SS-304 case is super-critical. As expected, the largest k_∞ occurs when the modules have no separation between each other. As the module pitch is increased after a certain value, k_∞ stops decreasing because the modules are too far apart to be coupled with adjacent modules. The SS-304 cases flatten out much faster than the Zr cases.

It has been shown that the 5% and 10% enriched SS-304 cases cannot go critical, so the two cases will not be carried forward; the 15% enriched SS-304 case will still be considered. The lower enriched SS-304 cases are subcritical due to the larger absorption cross section of SS-304 as compared to Zr.

A lower fuel enrichment is preferred, so the 5% enriched Zr case will also be carried forward. As a design choice, the higher enriched Zr cases will not be considered, but the options to increase fuel enrichment still exists.

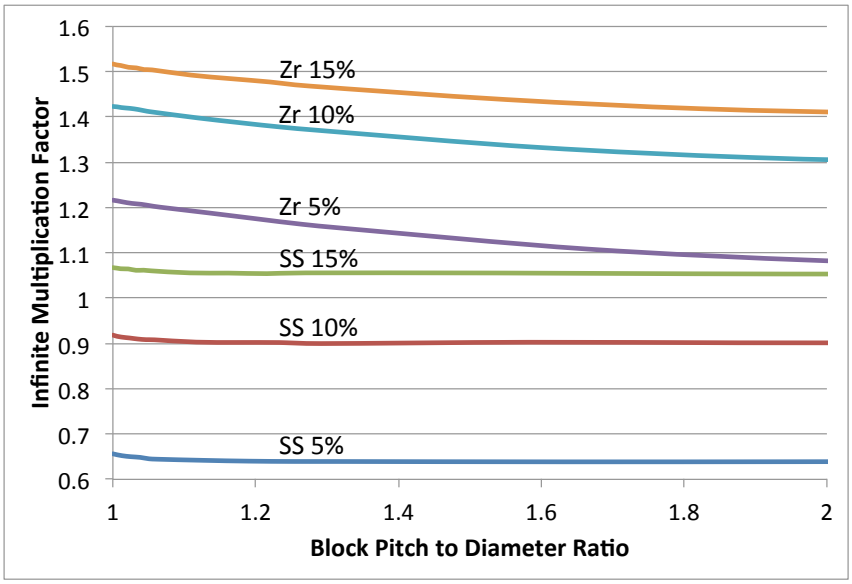

Fig. 4.4. k_∞ Dependence on Infinite Module Pitch to Diameter Ratios for Various ^{235}U Enrichments and Cladding Materials.

The module pitch to diameter ratio will bet set at 1.1 as at this PD_{mod}, k_∞ does not deviate much from the optimal value, and allows for enough space for easier manufacturing of the graphite blocks the modules sit in as well as possible control rod placement.

4.1.3 Finite Core

In reality, the core must be finite in all dimensions and include areas for the balance of plant components. The two cases to choose from are the Zr with 5% fuel enrichment case and SS-304 with 15% fuel enrichment case.

The set of blocks that make up the core is surrounded by a 1 m graphite radial reflector and and 1 m graphite axial lower reflector. Above the fuel is the upper plenum that is filled with CO_2. The core with 7 modules can be seen in Fig. 4.5.

The number of block rings (see Fig. 4.6 for description) and the height of the active fuel can be varied. To minimize leakage from each block, the active fuel height to

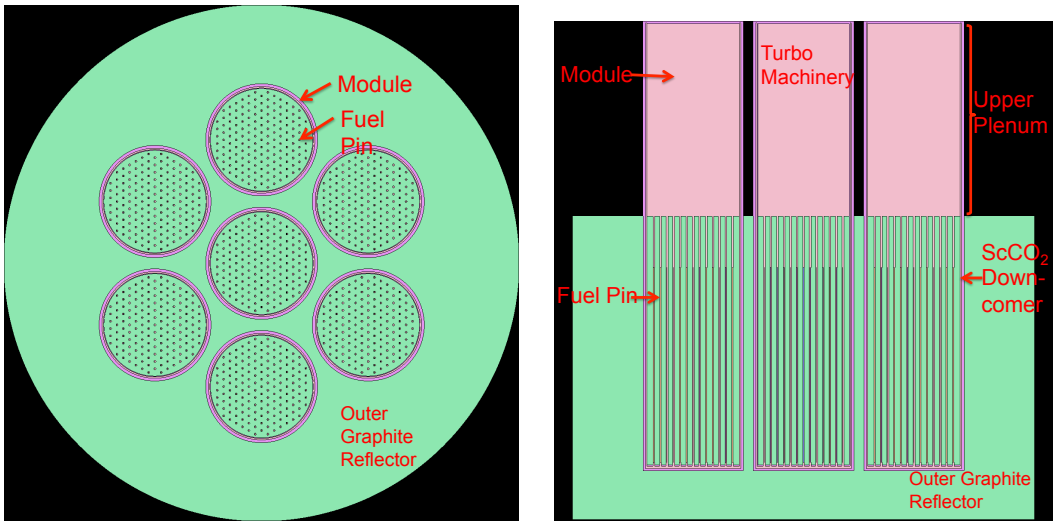

(a) Top View (b) Side View

Fig. 4.5. HT-IMMTR Geometry.

core diameter ratio is set to unity. This requirement was found to be impractical as once the number of block rings reaches 2, the fuel height is over 6 m. To alleviate the impracticality of the requirement, the fuel height is set to a constant 3 m. The impractical case was still investigated to be used as a comparison.

The effects of core size can be seen in Fig. 4.7. The core radii shown correspond to the Zr cases, and the connected points on the graph are a visual aid as it is not possible to have a fraction of a ring. The actual SS-304 radii are about 20% larger. The fuel height/diameter = 1 cases both have higher k_{eff} than the 3 m cases for configurations with 2 or more module rings. This is expected since more fuel in a geometry with less leakage will have a higher initial excess reactivity. The change in k_{eff} when comparing the fuel height/diameter = 1 cases and the 3 m cases is about .04, which is rather large so the fuel height will be increased to 4 m in future cases.

Each core can be made critical with 2 fuel rings, and adding more fuel rings shows an increase in k_{eff}, but the increase per fuel ring added decreases with more rings added. The number of rings metric can be a bit deceiving, as the number of

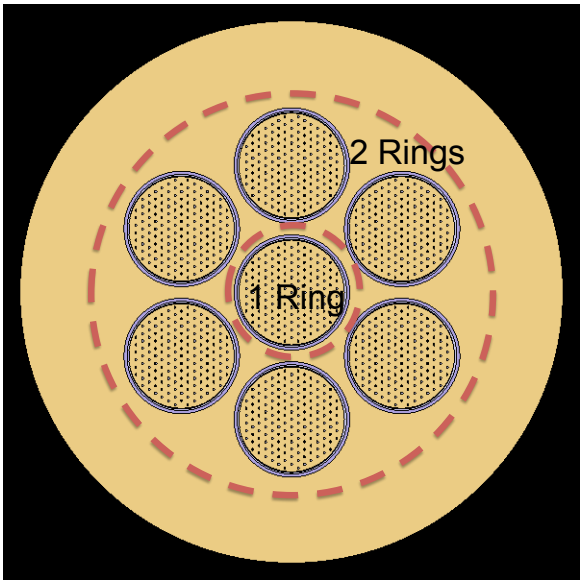

Fig. 4.6. Visual Description of Block Rings

modules added per ring added increases exponentially. A clearer representation of this is shown in Fig. 4.8. There are 19 blocks with 3 rings, adding a 4^{th} ring almost doubles the number of blocks, but only increases k_{eff} by about 0.02. This shows that neutronically, adding more blocks does not effect k_{eff} very much. However, the total number of blocks governs the total output power of the reactor, so it can be beneficial to have many block rings.

The Zr with 5% fuel enrichment case was found to have the largest initial excess reactivity and is chosen as the design case. The fuel height is also taken as 4m to increase the initial excess reactivity of all cases. To maintain a small reactor size, the 2 module ring case is used.

4.2 BeO Fuel Enrichment

The BeO fuel enrichment needs to be considered because BeO displaces fuel, which decreases the core lifetime, and is costly, which decreases economic viabil-

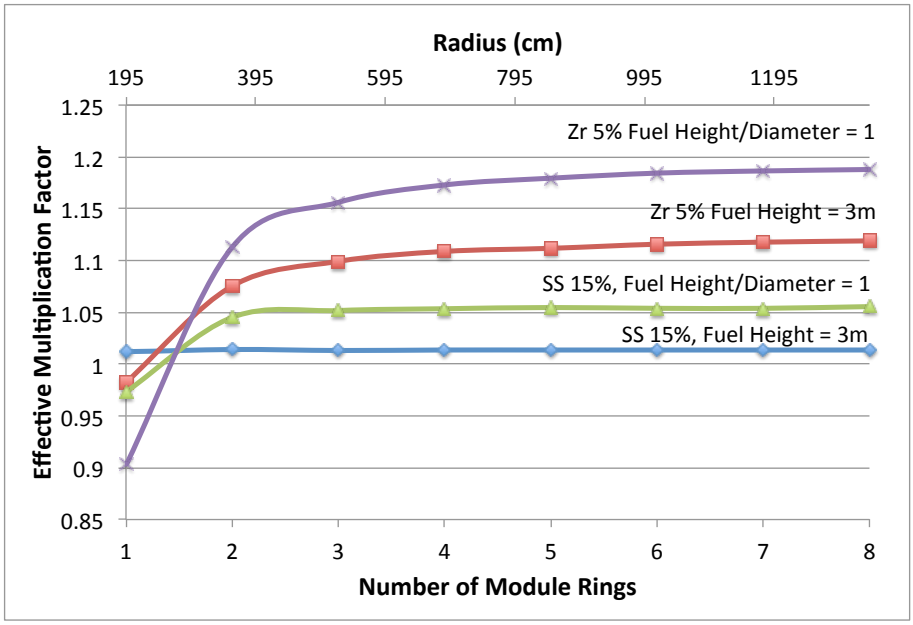

Fig. 4.7. Effects of Number of Module Rings on k_{eff}.

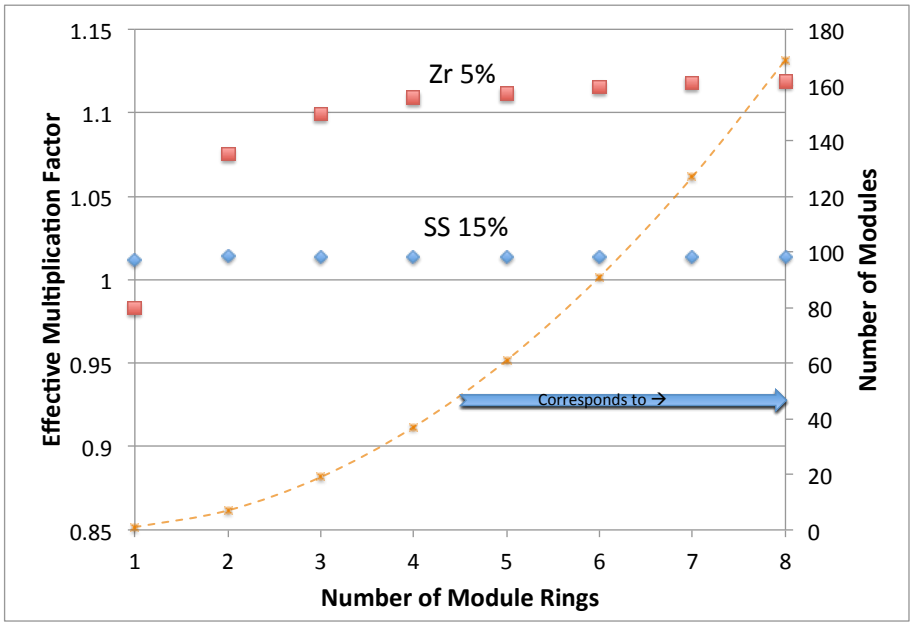

Fig. 4.8. Effect of Number of Modules Rings on k_{eff} and Core Size.

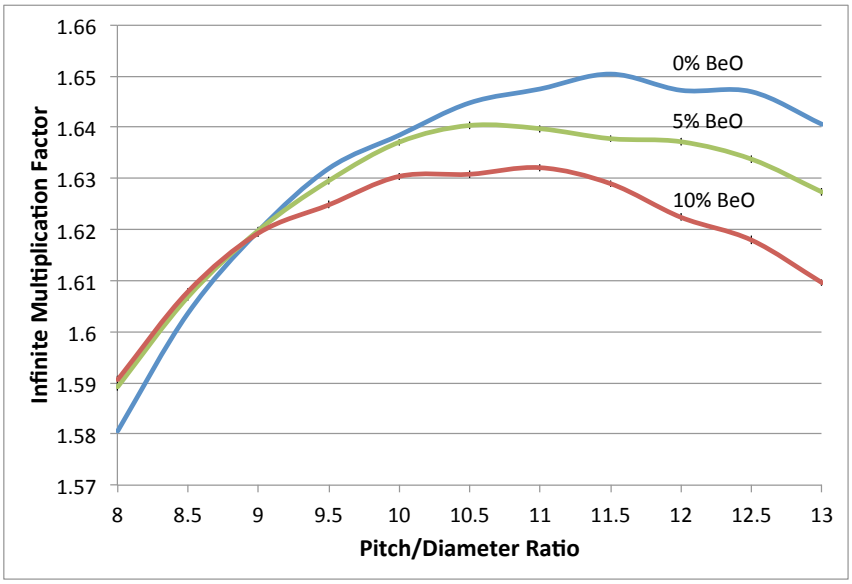

Fig. 4.9. Optimal Pitch Search for BeO Fuel.

ity (Kim et al., 2010). Fuel enriched with 5% and 10% BeO will be considered along with a 0% BeO control case to see the effects of BeO on the core lifetime. The fissile content of the fuel remains at 5 wt% ^{235}U.

4.2.1 Optimal Pitch to Diameter Ratio

Since the fuel changed, the optimal pitch for each case needs to be found. Using the same method as in Sec. 4.1.1, the pitch was varied to see effects on k_{eff}, and the results can be seen in Fig. 4.9. The more BeO present, the smaller the final core size will be since a tighter optimal pitch is obtained with more BeO.

4.2.2 Burnup Analysis

Figure 4.10 shows the burnup results of operating the core at 10 MW_{th} with 100% capacity for different BeO wt% additions. The burnup profile was found to be linear in all three cases so to save on computation time, the core lifetime were found

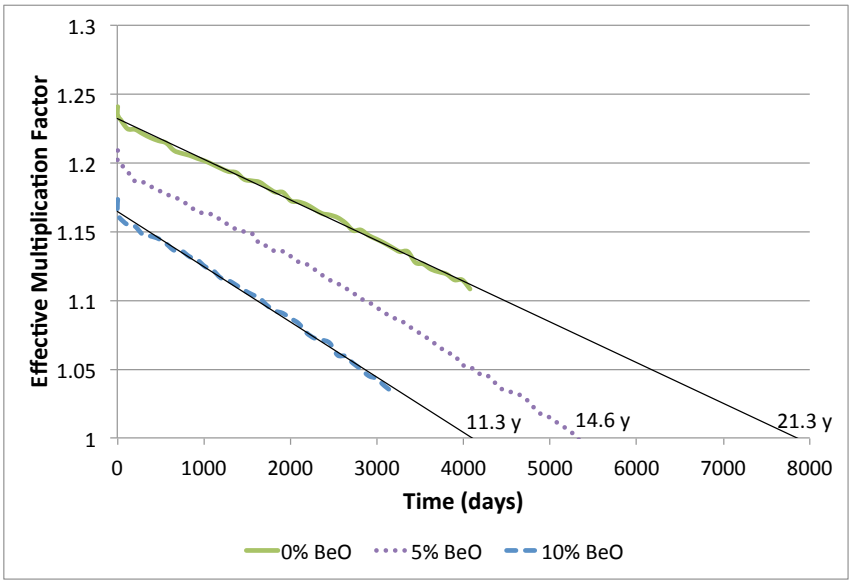

Fig. 4.10. Core Lifetimes for Different BeO Enrichments.

by linearly extrapolated acquired data to find when k_{eff}=1. When compared to the control, the 5% BeO case reduced the core lifetime by 6.7 years, or about 30% and the 10% BeO case showed a reduced core lifetime of 10 years or about 47%.

These results suggest the BeO fuel addition will not be economically viable since the fuel is more expensive and does not have as long of a core lifetime when compared to a BeO free case. However, that is not conclusive since a higher enrichment of U can offset the core lifetime deficiency while still maintaing the lower fuel temperatures that higher conductivity BeO fuel offers.

4.3 Flux and Power Distribution

For control and safety purposes it is important to know the flux and power distribution in the core. Regions with large power peaks have greater fission rates which leads to higher temperatures. The whole reactor must operate below certain temperature thresholds for safe operations, so the location and magnitude of these power

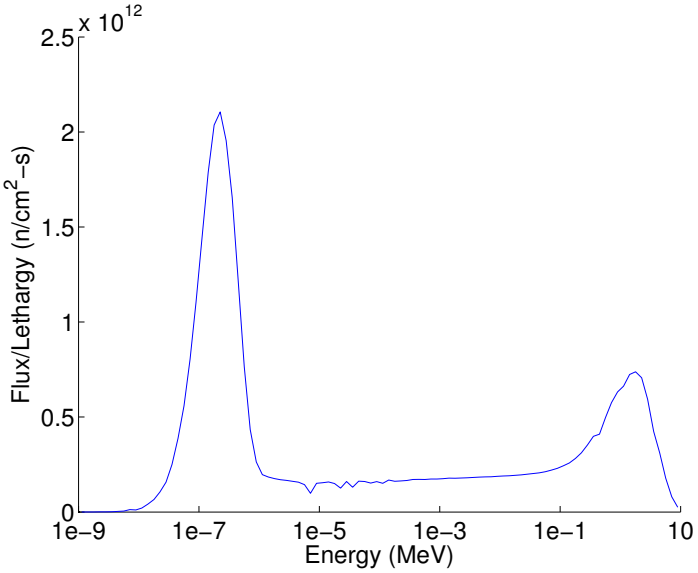

Fig. 4.11. Energy Dependent Neutron Flux in the Fuel Region.

peaks must be known. Regions of high flux are prime locations for control elements since control elements typically control the reactor by absorbing neutrons.

4.3.1 Energy Dependent Flux

The neutron energy spectrum of a reactor shows if a reactor is thermal, fast, or something in between. It is very important to know the neutron energies in a reactor, as reactor materials and control materials should be specified based on the spectrum. For example, a material that is a strong thermal neutron absorber maybe a good fast neutron reflector, so that material should not be used to control a fast reactor.

The neutron energy spectrum within the full core fuel region is shown in Fig. 4.11. The spectrum verifies that the reactor is a thermal reactor.

4.3.2 Flux Distribution

The neutron flux was tallied on a 300x300x60 grid and is plotted in Fig. 4.12. The central module has the largest radial neutron flux and the 6 outer modules have similar flux profiles to one another. There is a fairly large flux of neutrons between the modules, which shows that neutrons from different modules directly effect other modules. The axial core slice of Fig. 4.12(c) is taken through the centers of the central module and two outer modules. It shows that the central module as the largest axial flux, and the max flux within each module occurs near the centerline.

The core power distribution is needed because the neutron flux cannot reliably predict the location and magnitude of hot spots in the reactor. The power peaking takes into account actual fissions sites where heat is generated, whereas the flux only tracks neutron locations.

4.3.3 Power Distribution

The core power distribution was tallied on a 300x300x60 mesh. The power was found using the MT reaction mode "-6" for the total fission rate. Serpent is actually calculating the fission rate on the mesh by,

$$\text{Fission Rate} = \int_V \phi \Sigma_f dV,$$

where ϕ is the neutron scalar flux, Σ_f is the fuel fission cross section and V is the volume that the fuel is defined on. The power generated is directly proportional to the fission rate, so the fission rate, normalized to the power level is used as the power distribution. Serpent does not take into account gamma heating, so it does not find the true power distribution, but the fission rate is a very good approximation.

Since each mesh voxel will not necessarily encompass the whole fuel pin, some post processing of the data had to be done such that a pin-wise power distribution was

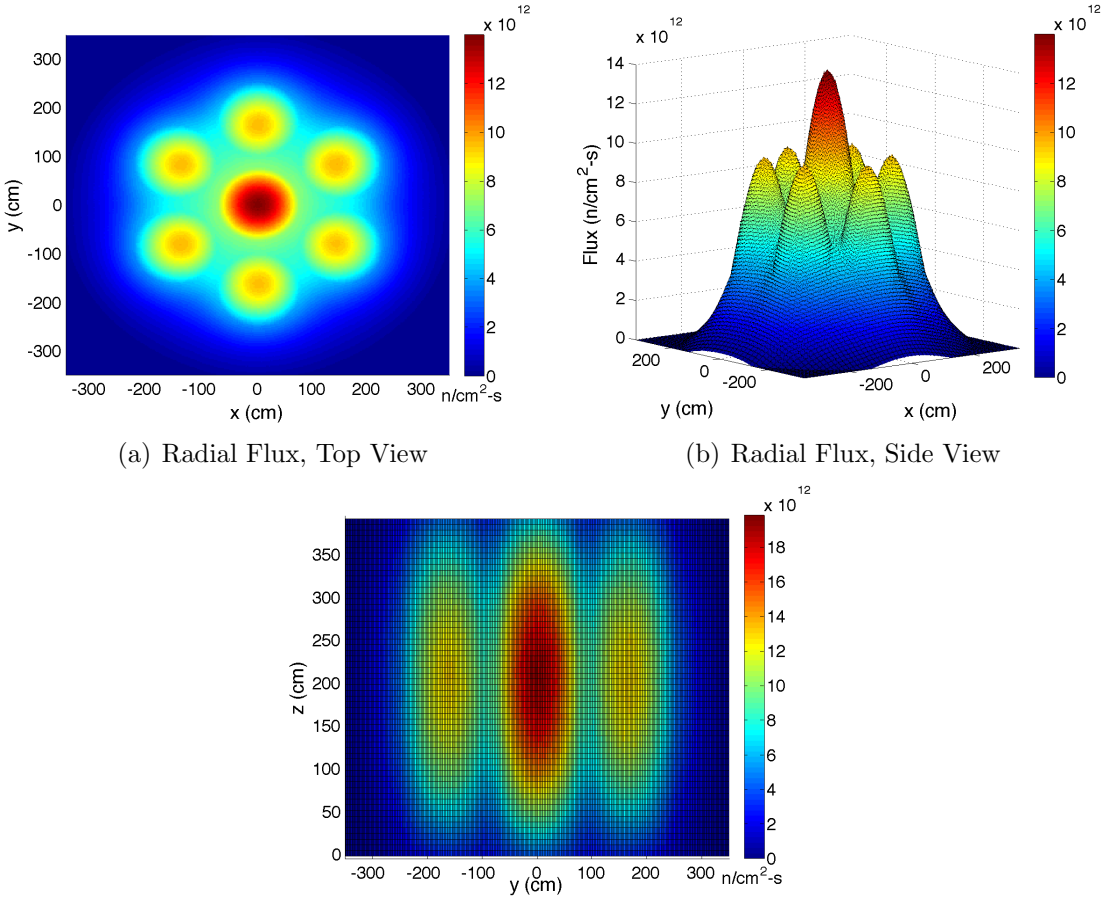

(a) Radial Flux, Top View

(b) Radial Flux, Side View

(c) Slice of Core Axial Neutron Flux

Fig. 4.12. Whole Core Neutron Flux.

generated. An example of the issue is shown in Fig. 4.13. Since the mesh intersects the fuel pin, 4 different regions are counted for 1 fuel pin, effectively creating 4 smaller pins instead of the actual single pin. If the fuel pin with the maximum power density was bisected then the true maximum would be lost. By adding up the bisected areas in post-processing, the actual power distribution is obtained.

The radial power distribution was obtained by integrating the full core power distribution over the fuel length, and is shown in Fig. 4.14. The side view, Fig. 4.14(a), shows many fuel pins so the distribution looks smeared, the important aspect to notice is that the side modules have a different power distribution than the central

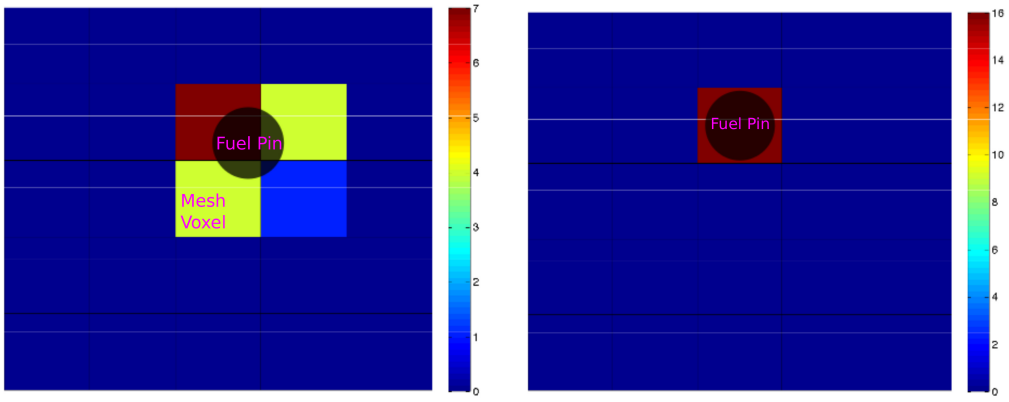

(a) Tabulated (b) Adjusted

Fig. 4.13. Adjusting the Tabulated Power Distribution to Obtain the Actual Distribution.

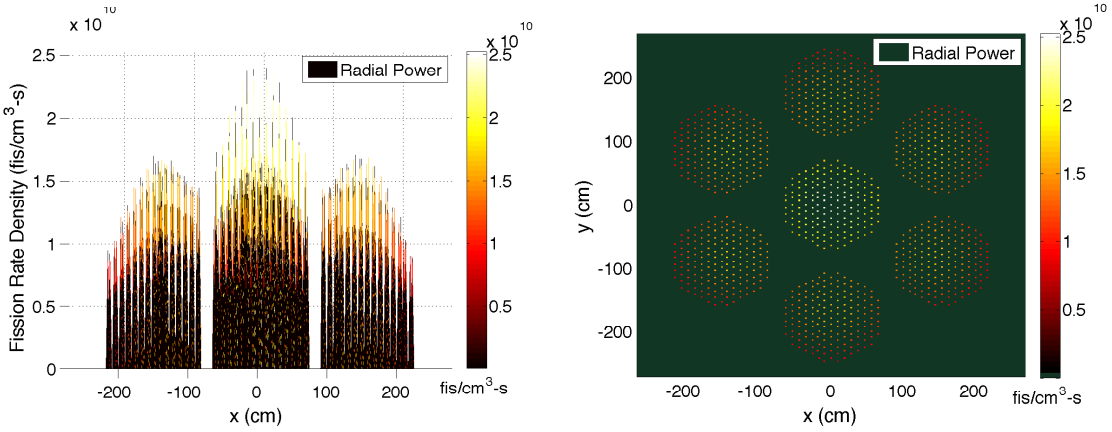

(a) Side View (b) Top View

Fig. 4.14. Radial Power Distribution.

module. The side modules peak with a bias towards the center. This is because there is a large influx of neutrons into the outer module from the center module, such that the fission rate is increased in the regions of the outer modules that is closest to the central module.

The top view, Fig. 4.14(b), shows the radial power distribution from a top down view. Each colored box represents a fuel pin, and its color represents the magnitude

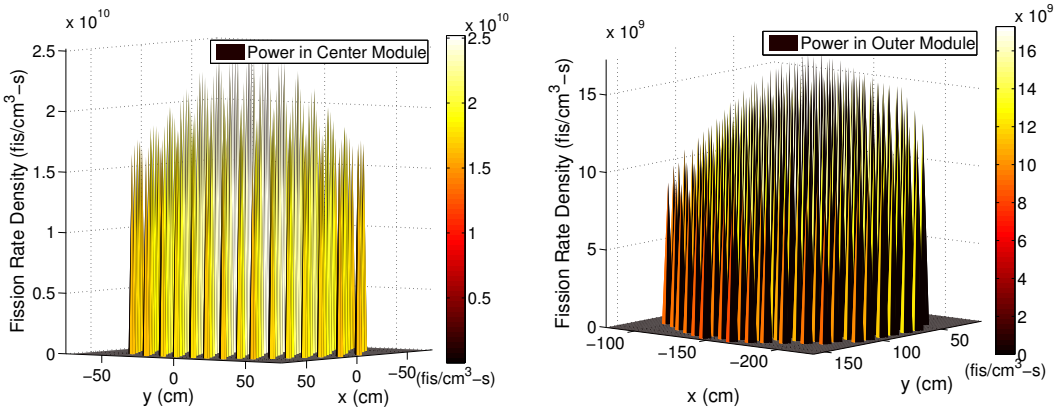

(a) Central Module (b) Outer Module

Fig. 4.15. Power Distribution Within Modules.

of the fission rate within that fuel pin. The maximum fission rate occurs in the center of the center module, while the minimum fission rate occurs in the outer peripheries of the outer modules. This image approximately shows the radial power distribution of the core; in reality there would be gamma heating that caused some of the fission heat to be deposited into the graphite and structural materials of the core. It is important to understand this because proper heat removal of the whole core–not just fuel pins is required.

The central and outer module power distribution is shown in Fig. 4.15. The distribution in the central module is symmetric around the module, whereas the outer modules are a bit skewed, having the peak off center. The heat generation profile (power profile) in the central module is different than the outer modules, so the thermal hydraulics of the modules will be different. This is another operating challenge that must be analyzed in a thermal hydraulics analysis.

The axial power distribution is shown in Fig. 4.16. It was obtained by integrating the full core power distribution over all radial positions. All the modules have similar parabolic axial power distributions, with the central module having a larger peak. The top of the core has a larger fission rate than the bottom of the core. This is

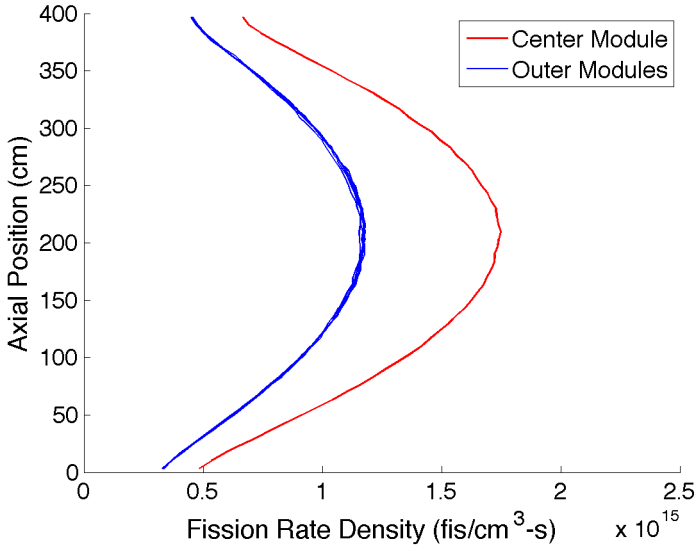

Fig. 4.16. Axial Power Distribution.

due to the bottom of the core being in proximity with the inner and outer pressure vessels which is an absorber that decreases the effects of the lower reflector. This distribution can be used in a hot channel thermal hydraulics code.

Power Peaking

The power peaking factor is defined as the ratio between the maximum fission rate and the average fission rate defined over a volume. The peaking factor is typically used as a safety factor to give the upper limit values of normal operating conditions. The power peaking factor was computed by

$$PF = \frac{\Sigma_f \phi_{max}}{\int_V dV \Sigma_f \phi}, \tag{4.3}$$

where PF is the peaking factor, ϕ is the neutron scalar flux, Σ_f is the macroscopic fission cross section, and V is the volume that the peaking factor is defined on. The volume V and definition of the flux, ϕ, changes depending on the peaking factor

Table 4.2
Full Core Peaking Factors.

Module #	Module	Radial	Axial
1	1.201604 ± 0.001711	1.278948 ± 0.078773	1.346873 ± 0.079359
2	1.206845 ± 0.001712	1.280608 ± 0.074365	1.340275 ± 0.078621
3	1.190641 ± 0.001706	1.272790 ± 0.078148	1.331896 ± 0.078561
4	1.731163 ± 0.002007	1.250092 ± 0.075209	1.344162 ± 0.062970
5	1.190528 ± 0.001703	1.277587 ± 0.074711	1.342058 ± 0.079265
6	1.202404 ± 0.001707	1.285174 ± 0.074861	1.340927 ± 0.079017
7	1.199129 ± 0.001703	1.288922 ± 0.079784	1.342908 ± 0.079338

in question. The axial module peaking factor volume is defined on a single module using $\phi(z)$. The radial module peaking factor volume is defined on a single module using $\phi(r)$. The module peaking factor volume is defined over the volume of all the modules using $\phi(r)$. The module peaking factor gives the hottest module as compared to the average, the axial module peaking factor gives the hottest axial zone within a module, and the radial module peaking factor gives the hottest radial zone within a module.

The power distributions obtained in Sec. 4.3.3 were used in Eq. 4.3 to find the peaking factors shown in Tab. 4.2. The outer modules do not deviate from the core average by more than about 20%, whereas the central module is 75% greater than the average. This large difference would require that the cooling conditions of the central module be quite different than the outer modules. If the core peaking could be controlled with control rods, then a more homogenous operating conditions could be achieved. The radial peaking factor is about the same in each module. This result is not to be misunderstood as the radial power distribution being the same in every module (see Fig. 4.14(a) for power shape). The axial peaking factors are also about the same in each module.

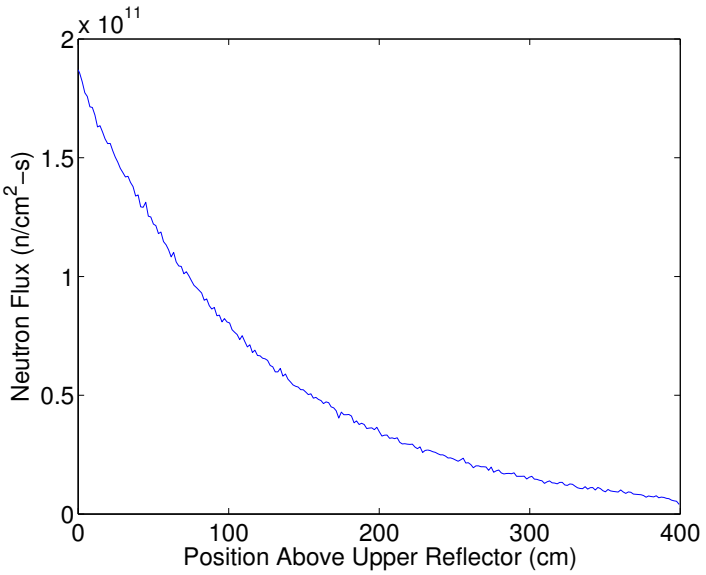

Fig. 4.17. Flux in the Reactor Upper Plenum.

4.3.4 Flux in BOP Area

The neutron fluence to the upper reactor area is important since the upper area contains BOP machinery that must be able to operating in a high radiation environment. The neutron flux to the upper regions of the 7 modules is shown in Fig. 4.17. This information along with the composition of the turbo-machinery should be used to predict the amount of radiation damage that would occur during operation. If needed, radiation shielding can be added to the upper plenum to limit neutron fluence to BOP equipment.

4.4 Reactor Kinetics Parameters

The reactor kinetics parameters are typically used in the Point Reactor Kinetics Equations for use in simple transient analysis or control theory. They can also be used as a simple basis to compare different reactors. The kinetics parameters for the HT-IMMTR are shown in Table 4.3.

Table 4.3
Reactor Kinetics Parameters.

Parameter	Value	Notes
β	0.00665	Delayed Neutron Fraction
Λ	1.17235E-03 s	Mean Generation (Reproduction) Time
l	1.41546E-03 s	Prompt (Total) Neutron Lifetime

It is also impossible to compare different reactors using only one metric as a reference. The reactor kinetics parameters allow for a good basis of comparison, although the set of parameters is still not enough to conclusively fully compare different reactors. Typically, the neutron lifetime and delayed neutron fraction reveal the difficulty of controlling a reactor. A short neutron lifetime means more neutron generations occur within a unit time frame when compared to a reactor with longer neutron lifetime. A smaller delayed neutron fraction means more neutrons are born prompt when compared to a reactor with a larger delayed neutron fraction. A shorter neutron lifetime and smaller delayed neutron fraction means a transient will propagate quickly, such that any control devices would have to act on fast time scales.

The delayed neutron fraction for the HT-IMMTR is typical of LEU systems. The prompt neutron lifetime of the system is long compared to an LWR since graphite requires more collisions to thermalize neutrons than water does, so the average time between fissions is longer. These parameters are inductive of a relatively easy to control reactor since perturbations to the reactor would not propagate on really short time scales. However, the modular nature of the reactor still presents control issues.

4.5 Reactivity Coefficients

Reactivity coefficients tell how the reactivity of the reactor system changes with a change in the reactor such as the fuel temperature increasing. The coefficients are generally nonlinear and are used in transient and safety analyses.

In general, reactivity coefficients depend on many factors such as power level, temperature, density, and pressure. The reactivity coefficient from temperature is usually of interest since a negative coefficient is necessary for inherently safe operation. A negative temperature coefficient of reactivity means that if the temperature of the materials in the reactor increases, the multiplication factor of the core decreases.

The coefficient of reactivity was found by

$$\alpha_x = \frac{\frac{1}{k_1} - \frac{1}{k_2}}{T_2 - T_1}, \tag{4.4}$$

where standard notation is used along with the subscripts 1 and 2 referring to the temperature steps that the calculations were performed at and x is the mechanism of reactivity change (e.g., fuel or moderator temperature change). While the specific mechanism of change, x, is changed, all other reactor parameters should be held constant. The reactivity coefficients reported are taken to be at the average temperature between the two evaluated temperatures.

Neutron cross section data libraries are temperature dependent and each library corresponds to a different temperature. To use Eq. (4.4) with Serpent, the appropriate data libraries were called when defining the materials in the input. For time dependent cases, the time dependent fuel vectors found in the burnup analysis were inputed. Since the coolant density changes appreciably with temperature, the appropriate densities at different temperatures had to be inputed when evaluating the coolant temperature coefficient of reactivity.

The nonlinear dependence of the coefficients on reactor operating conditions means many data points at different conditions must be found. The fuel temperature, moderator temperature, and coolant temperature coefficient of reactivity were evaluated at several temperatures and times. The coefficients are shown in Fig. 4.18.

The graphite temperature coefficient is large and negative, meaning an increase in graphite temperature will add negative reactivity. The strong negative temperature feedback and large heat capacity of graphite is beneficial to the safety of the reactor during an accident scenario. The graphite can serve as a temporary heat sink for the fuel in the event of a LOCA or LOFA. As the graphite temperature rises, negative reactivity is inserted into the core, which makes the core subcritical. The presence of graphite in the core allows for more time for operators to react to an emergency.

The fuel temperature coefficient is also large and negative, although it is smaller in magnitude than the graphite coefficient. This is a little misleading as the fuel temperature can change very quickly, whereas graphite temperature changes happen on much longer time scales. This means the fuel temperature coefficient has a much more instantaneous effect and is even more important on reactor safety than the moderator coefficient. A large increase in fuel temperature, given the fuel does not melt, would give rise to a strong instantaneous negative reactivity insertion which will decrease the fission rate, and give time for the fuel to be properly cooled.

The moderator temperature coefficient is very small compared to the fuel and graphite coefficients. The $ScCO_2$ in the system does not interact much neutronically with the core, although it does have some effect. Within error bars, the coolant temperature reactivity coefficients are negative, although at some states, the coolant may add a small positive insertion. The coolant neutronic properties are important to know for a LOFA analysis since the coolant temperature would increase if forced convection was stopped. If a positive insertion was added by the coolant, the negative fuel and graphite temperature coefficients would counter balance it.

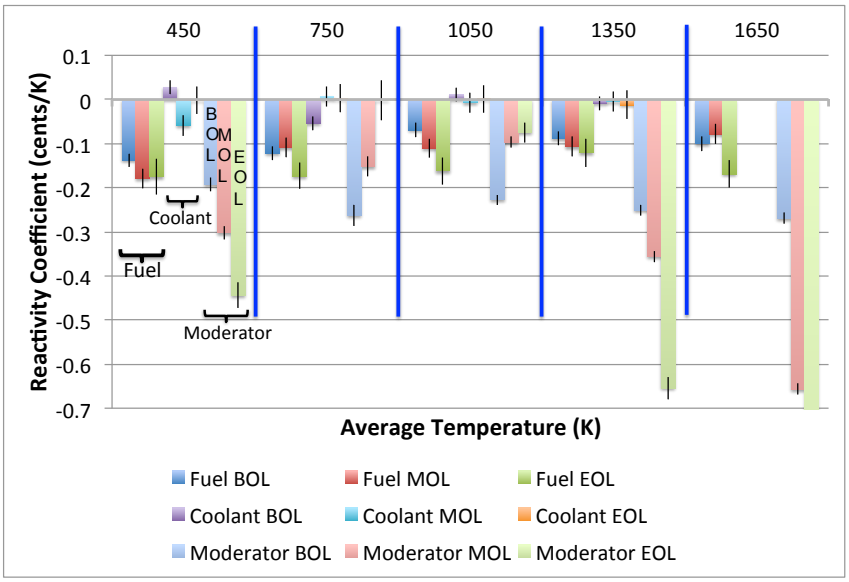

Fig. 4.18. Fuel, Moderator and Coolant Temperature Coefficients of Reactivity.

4.6 Outer Reflector Size Optimization

In efforts to reduce the total core size of the core, the effects of the size of the outer graphite reflector were investigated. The reflector thickness was changed and k_{eff} was found; results are shown in Fig. 4.19. After about 50 cm, adding more graphite did not change the multiplication factor much. This means that the core size can be reduced by 1 m, without changing the lifetime very much, when compared to the above design case.

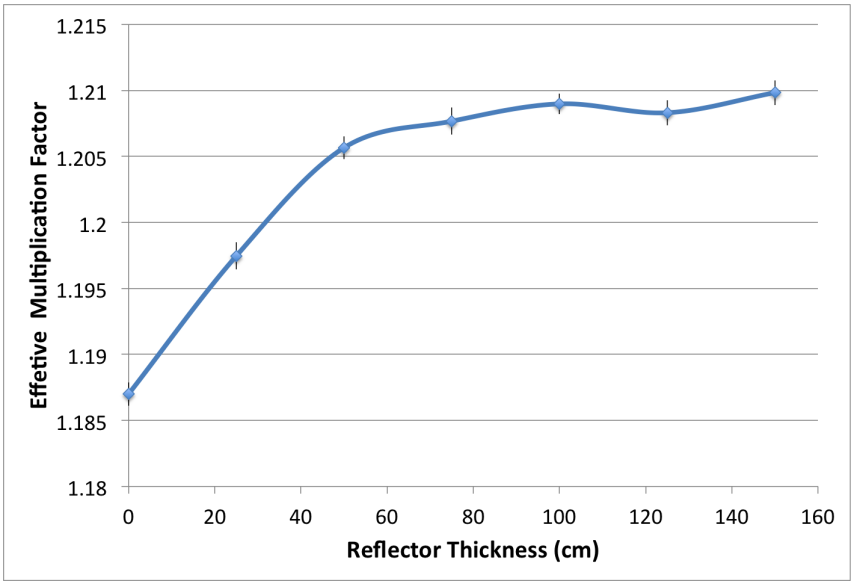

Fig. 4.19. Reflector Size Effects on k_{eff}.

5. MODULARITY STUDY

With an established design basis, the modularity of the reactor can be further investigated. Battery type fuel replacement and shuffling is modeled to find out if the core lifetime can be increased. Several accident scenarios will also be modeled. The effects on creating a core with fuel dispersed in several modules rather than one large module is also analyzed.

The standard to compare results to is the design with 5% BeO enhanced fuel with 5% ^{235}U enrichment and Zr cladding in a 2 ring configuration with 4 m fuel. This configurations achieves a lifetime of 5335 days with a burnup of 18.8455 GWd/tHM.

5.1 Module Shuffling

Intra-modular fuel reshuffling is impractical and against the design basis of requiring modules that are sealed during the core lifetime. Moving the modules themselves is feasible and can potentially extend the core lifetime.

An interesting shuffling pattern is to rotate each of the outer modules 180 degrees at the middle of life. Within a module, since the power distribution is higher towards the center of the core than the periphery, the fuel on the periphery should have less burnup than the fuel towards the center.

Two burnup regions were used in each module and the model was ran until the EOL condition so fuel vectors at many different time steps were available. The module rotations were modeled by swapping the location of modules that were opposite of each other. This is shown in Fig. 5.1; within each letter group, the unprimed locations move to the primed locations and primed locations to the unprimed. This made the fuel that was towards the center during operation move to the periphery, and the peripheral fuel move to the center. During actual operational conditions, the modules could simply be rotated on their own axis.

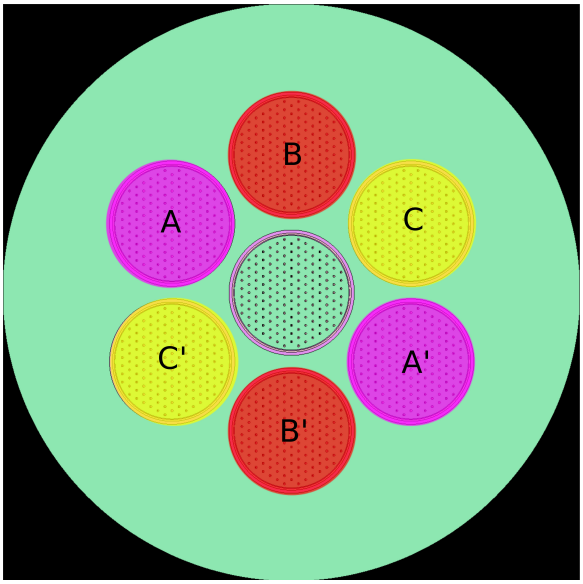

Fig. 5.1. Top View of Reactor With Modules Label.

It was found that rotating each module at 2455 days did not increase the core lifetime. This is likely from the burnup distribution within a module being about the same at any radius, so turning the module has little to no effect. This result could also be an artifact of not having enough burn regions to capture burnup effects in the calculation. Since defining each fuel pin as a separate burnable material is very RAM expensive, it was not possible to do with the computation resources available.

If there was a large burnup gradient present, it would show at the EOL. A module rotation toward the EOL did not increase the core lifetime, so either there is not a large burnup gradient in the core or the model is not of high enough fidelity to capture the burnup gradient.

5.2 Module Replacement Refueling

5.2.1 MOL Module Replacement

Replacing the central module at the MOL may increase the core lifetime since the central module has the highest burnup, and the introduction of fresh fuel may allow a higher burnup of the outer modules.

The central module was replaced with a fresh module at 2455 days, which resulted in a burnup increase to 20.317 GWd/tHM and core lifetime extension to 5810 days, which is about 1.25 years more than the standard case. This increase in lifetime is not economically appealing since the cost of adding another module would likely out weigh the extra profit from operating for 1.25 more years.

5.2.2 Batch Module Refueling

Typical LWRs replace fuel in batches to increase the total burnup of the fuel. This idea is implemented into the HT-IMMTR by creating an inner and outer batch region. The inner region consists of the central module, which, during operations, is subjected to a higher burnup than the outer modules. The outer region consists of the 6 outer modules.

The core was allowed to run to the EOL, 5335 days. Then the central module was replaced, leaving the outer modules in place and the core was ran until the EOL case, which took 1195 days. The outer modules were then replaced and the core ran for 4435 days. In total, using batch module refueling the core ran for 10965 days, compared to 10670 days if all the modules were replaced at once. That is a 1 year increase of total life time.

5.3 Single Reflected Module Performance

A single subcritical module can be made critical when surrounded by a large graphite reflector. To see if having the modules in a ring configuration actually effects the core lifetime, the single module case was burned at 10 MW.

Burning a single, properly reflected module at 10 MW resulted in a core lifetime of 1.25 years. So, 7 discrete modules operating at a total capacity of 70 MW would last 1.25 years. When put into the 2 ring configuration, 7 modules producing 70 MW lasts 2.4 years. This shows a clear benefit of the multi-modular configuration on core lifetime.

5.4 One Large Module Performance

From a neutronic perspective, the longest core lifetime will be achieved when absorbing materials, such as the module materials or the extra inter-modular graphite are not present. This can be achieved by putting all the fuel in one module. Although this configuration would be more difficult to control, and would be large and difficult to manufacture, the core lifetime deficit between fuel in 7 modules and fuel in 1 module can be a good metric to evaluate the usefulness of modularity.

With all the fuel in one module (see Fig. 5.2), operating at 10 MW, a core lifetime of about 32 years is achieved. This means that splitting the fuel into 7 modules decreases the core lifetime by a factor of about 2. Although this is a large difference, the advantages of a module core far out-weigh this core lifetime deficient.

In a one large module configuration, the fuel and the reactor materials would likely not survive such a long irradiation time. This large configuration would be difficult to construct since the reactor pressure vessels would be very large. The ability to use modules for different purposes within a single configuration would be lost, e.g., 3 modules for heat generation and 4 for power production. The initial k_{eff} of the one large module configuration is 1.48392 ± 0.00092, which is about 68$

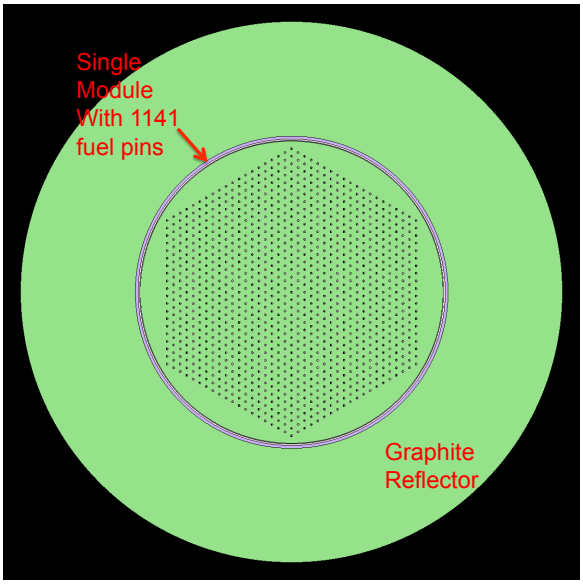

Fig. 5.2. Geometry of One Large Module.

of excess reactivity that would need to be controlled–not an simple task and would likely be unsafe. It has therefore been shown that the several module approach is a better approach than having one large module.

5.5 Removing Modules During Operation

The reactivity worth of different modules were found by removing a module and comparing the k_{eff} to a normally operating configuration. This shows the effects of removing a single module from the system. Although removing a module during operation would be difficult, there is a possibility of this occurring. A removal method can be implemented by design to either repair or replace a module.

A k_{eff} search was made on a configuration with a single module missing. In one case, the central module was removed, and in another case, an outer module was removed. Both cases were conducted at the BOL and the MOL (2455 days). The reactivity inserted for each case is shown in Table 5.1.

Table 5.1
Reactivity Changes Due to Single Module Removal.

Method of Change	$\rho\left(\frac{\Delta k}{k}\right)$	ρ (\$)
Remove Central Module	-0.0161 ± 0.0007	-2.37 ± 0.10
Remove Side Module	-0.0059 ± 0.0010	-0.87 ± 0.14
Remove Central Module at MOL	-0.0151 ± 0.0014	-2.22 ± 0.20
Remove Side Module at MOL	-0.0049 ± 0.0013	-0.73 ± 0.19

The reactivity worths for the central module is larger than the side module since the central module has a larger fission rate, and when removed will effect the reactor more than a side module removal. The reactivity worth at the MOL cannot be conclusively compared with the BOL case due to large errors. It is expected that the worth of each module is less at the MOL, although it is not substantially less since a lot of fissile content is still present. Removing a module during operation would cause the reactor to shutdown unless proper control rod adjustments were made.

5.6 Accidents

In the event of an accident, the ability for a reactor to safely shutdown and maintain proper decay heat removal is very important. Several accident scenarios were created and the neutronic response of the reactor to these accidents was characterized.

5.6.1 Room Temperature, Single Module Criticality

A unique design feature of the IMMTR is that each module is subcritical individually. To verify this, a single module at room temperature (300K) was modeled without an outer graphite reflector. Any temperature higher than room temperature

will have a lower k_{eff}. A k_{eff} of 0.978605 ± 0.000401 was calculated, showing that each module is indeed subcritical.

There is still the possibility of the reactor coming into contact with a good reflector such that a critical geometry is made.

5.6.2 Water Accident

Each module is designed to be able to be transported by barge. No transport method is perfect, so the barge has the possibility of sinking. If a barge with a HT-IMMTR were to sink, the module would be surrounded by a water reflector. Modeling this scenario, a k_{eff} of 0.978672 ± 0.00116 was found, so the addition of a water reflector could not make a module become critical.

In the event of an accident where the barge sinks, the module could be damaged such that all coolant channels are filled with water. The reactor must not be able to become critical or else the barge would not be a safe transport method. A criticality search calculation with the primary coolant replaced with water and the module surrounded by water showed a k_{eff} of 0.846153 ± 0.000381, which means that in the event of a water-accident, the reactor will remain subcritical. Since the water adds moderation to the core, the core would now be over-moderated, but since it's subcritical, there is no criticality issue.

5.6.3 LOCA Analysis

A loss of coolant accident (LOCA) is an accident case where there is a break in the reactor cooling system and coolant is lost from the reactor. The HT-IMMTR is less prone to this sort of accident since large amounts of piping are not in the design, but a rupture in the pressure vessels is still possible.

A LOCA of the HT-IMMTR was modeled by replacing the $ScCO_2$ coolant with void. The temperature changes that would result from the LOCA are not modeled.

Table 5.2
Reactivity Changes Due to a LOCA.

Scenario	$\rho\left(\frac{\Delta k}{k}\right)$	ρ (\$)
LOCA of Central Module	0.0000 ± 0.0002	0.00 ± 0.04
LOCA of A' Side Module	-0.0001 ± 0.0002	-0.01 ± 0.04
LOCA of Central Module at MOL	-0.0023 ± 0.0011	-0.37 ± 0.18
LOCA of A' Side Module at MOL	-0.0063 ± 0.0013	-1.02 ± 0.21

Table 5.2 shows a LOCA for a single module would add a small negative reactivity into the system. Within the error bars given, it is possible that a LOCA can add a small amount positive reactivity. In either case, the reactivity inserted is not enough to shutdown the reactor since the LOCA reactivity inserted would be counterbalanced by the fuel temperature coefficient of reactivity. A positive insertion would increase fuel temperature which would add negative reactivity, and a negative insertion would decrease fuel temperature which would add positive reactivity. Control rods would be needed to shutdown the reactor. An emergency cooling mechanism must also be implemented to insure the integrity of the reactor. After a LOCA and SCRAM, the graphite in the system can act as a good heat sink for short times until proper cooling of decay heat can be established. A secondary cooling system would need to be implemented to maintain safety during a LOCA.

5.6.4 LOFA Discussion

A loss of flow accident (LOFA) is an accident where the forced flow of the coolant is lost. This can lead to unsafe conditions since heat is not properly being removed from the reactor by forced convection. The reactor would be SCRAM'ed in response to a LOFA, so the amount of heat being produced would be much less than when operating. With the reduced heat production, natural convection of $ScCO_2$ maybe

able to convect heat away from the fuel and keep the core safely cooled. The physics of this would need to be modeled by a thermal hydraulics analysis.

5.7 Control Elements

To maintain control of the core throughout the lifetime, control rods must be placed in the core. Control rods also provide a means to shutdown the reactor in the event of an emergency. There are several types of control rods that can be implemented in this reactor.

Inter-modular and intra-modular control rods are both feasible solutions. Intra-modular rods would either displace fuel or reflector within the modules, and would also add extra control rod movement machinery to a already tight configuration. Since intra-modular control rods would make the design complex, they will not be considered.

Criticality of the subcritical modules is achieved when several modules are brought into proximity of one another. The physical reason for this is that neutrons are leaking out of each core. When only a single module is present, any leakage of a neutron is a loss of a neutron from the system. With several modules close to one another, neutrons leaked out of one module can enter into adjacent modules, so the neutron is not lost from the system. A method of controlling the core is to control the leakage using inter-modular control rods. Since each module is subcritical on its own, control rods can act as a neutron barrier that separates all the modules. Depending on the degree of coupling between the modules, a few control pins can be placed throughout the graphite or large cylindrical control shells can be placed around each module.

The control material used is made of 80-15-5 Ag-In-Cd (80% Ag, 15% In, 5% Cd). This material is effective at a large spectrum of neutron energies and is typically used in LWRs. This analysis is performed on a fresh core.

5.7.1 Control Pins

Six 3 cm control pins were placed around the central module, but these were unable to make the core go subcritical at BOL. This is attributed to the fact that the graphite reflectors help make the critical configuration, so the reflection must be reduced to change the core multiplication factor appreciably.

To reduce the amount of reflection, cylindrical control shells were placed around each of the modules. The control shell placement can be seen in Fig. 5.3. The control shells are the same height as the fuel, 4m, and their thicknesses and positions need investigation.

5.7.2 Control Shell Thickness

The thickness of the shell helps determine the reactivity worth of the shell and its lifetime. Therefore, the thickness used should be based on neutronics and economics. The control shell can only take a finite neutron fluence before needing to be replaced so a larger thickness of shell, will result in a longer shell lifetime, but more control material would result in a higher cost of control material. The longest expected control shell lifetime is preferred since the reactor is expected to be capable of autonomous operation. However, if the shell gets too large, the control shell would be have too much negative worth, making the reactor harder to control. To find the effect of shell thickness on k_{eff}, the shell thickness was varied and the results are shown in Fig. 5.4. All shells were 100% inserted and placed .1 cm from the modules. The difference between a .1 cm and .5 cm shell is very large compared to the difference between a .5 cm and 3 cm shell. A 2 cm shell was chosen since this provides for a larger shell that should be able to withstand a larger fluence, and is neutronically effective.

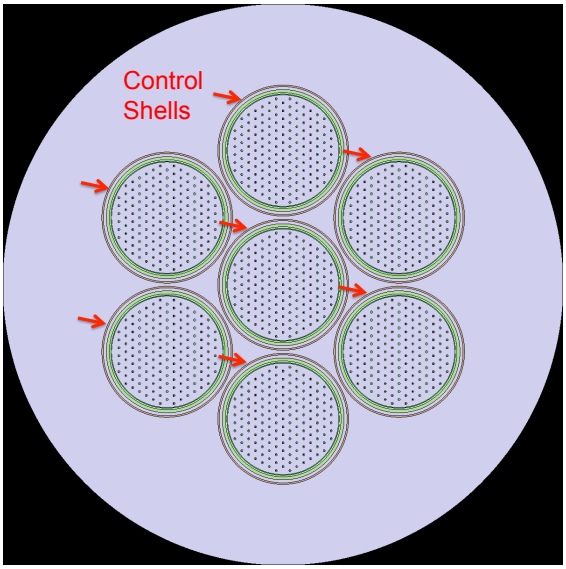

(a) Top View

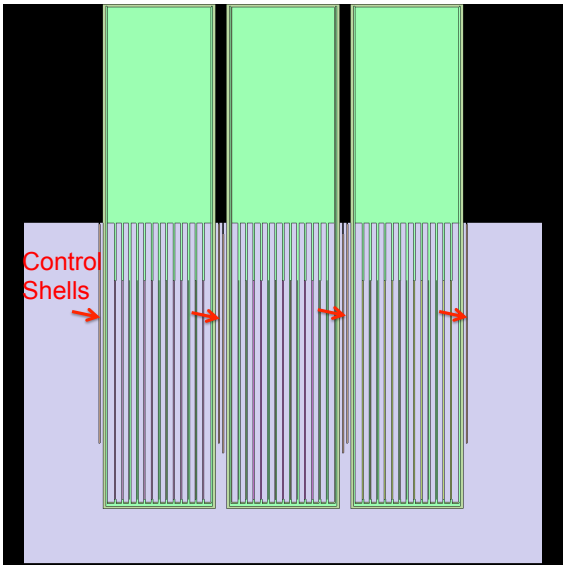

(b) Side View

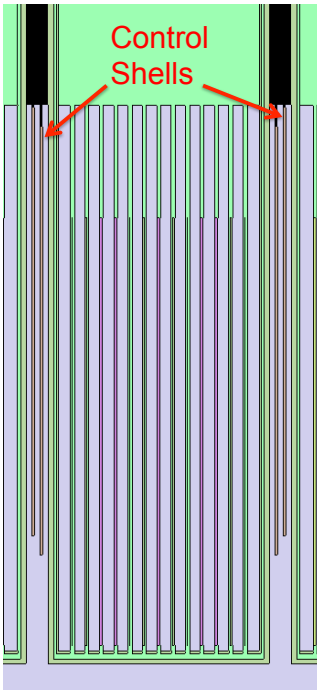

(c) Zoomed Side View of Central Module

Fig. 5.3. Control Shell Locations.

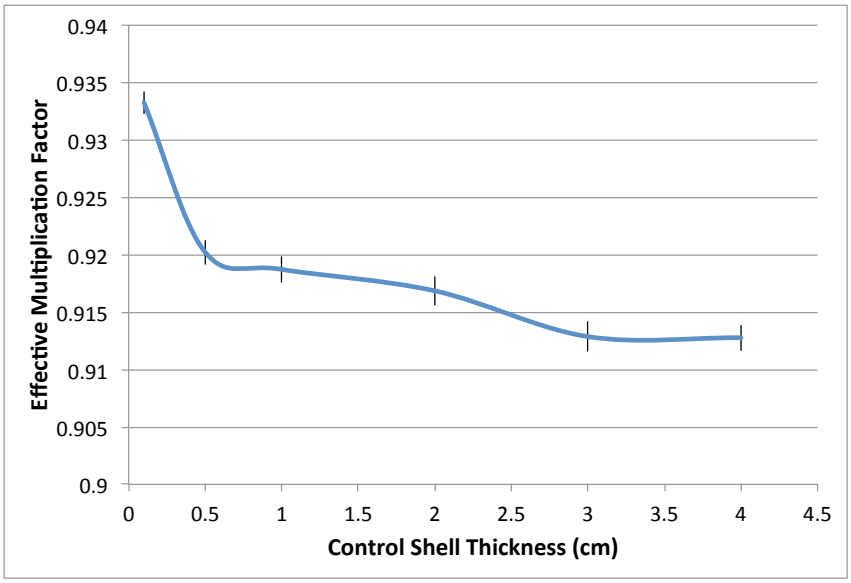

Fig. 5.4. Control Rod Size Search.

5.7.3 Control Shell Location

The location of the shells relative to a module will change the reactivity worth of the shells as well as the power distribution in the core. Control shells placed very close to the modules could distort the flux near the module edges and cause large flux gradients that would lead to higher peaking factors and uneven burnup. To investigate, the peaking factors and power distributions of a core with 2 cm thick control shells placed flush with the modules and a core with 2 cm thick control shells placed 4 cm from the module radius are compared. The inner shell was 78% inserted and the outer shells were 73.5% inserted. These configuration made to be critical within a few % of $k_{eff} = 1$

Table 5.3 shows the peaking factors for the comparison. The module peaking factors for the 4 cm case are larger than the flush case, the radial peaking factors are comparable, and the axial peaking factors are lower. The axial and radial power distributions are compared in Fig. 5.5. The radial distributions look similar to one another. Since this is an axially integrated quantity, it does not show that the radial

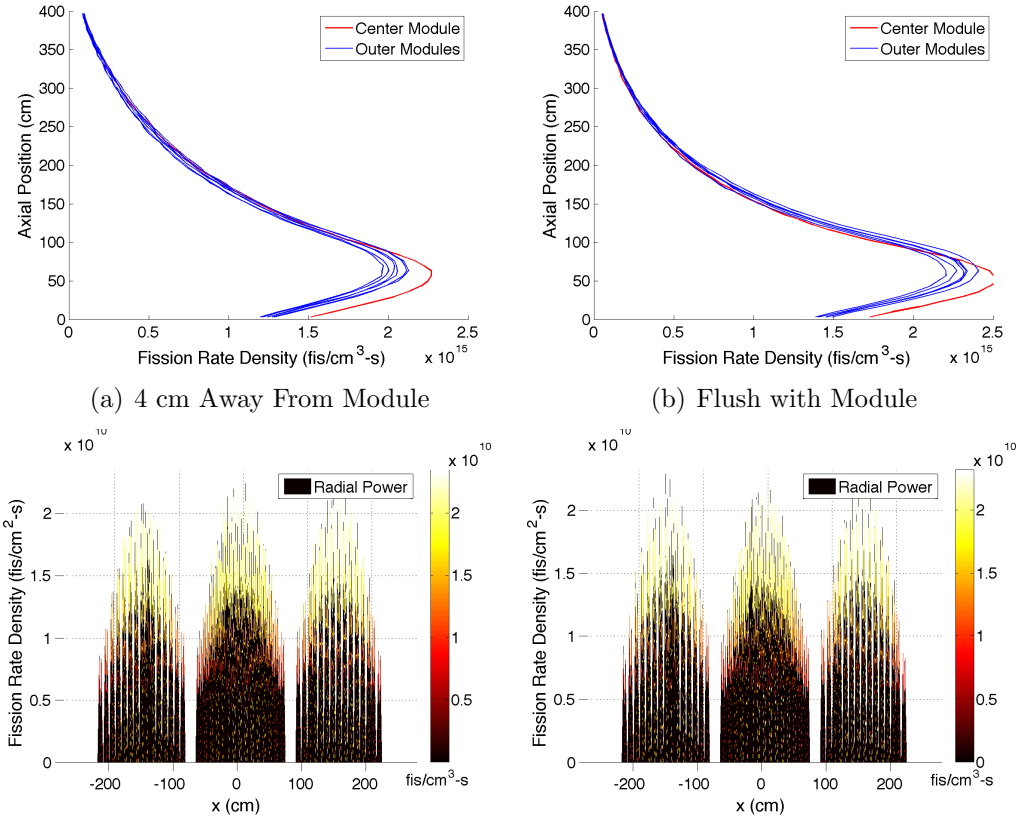

(a) 4 cm Away From Module

(b) Flush with Module

(c) 4 cm Away From Module

(d) Flush with Module

Fig. 5.5. Axial and Radial Power Distribution Comparison for Different Control Shell Locations.

power distribution is much more dense towards the lower part of the core than the higher part, but the axial distribution does show this. The power shape is skewed towards the bottom of the core in both cases. The 4 cm case has a lower axial peaking factor than the flush case confirming that the position of the control shells does effect the power distribution and can cause higher peaking.

Control shells placed further out are more effective when the outer shells are fully inserted and the inner shell fully withdrawn, whereas if all shells were fully inserted, shells placed closer to the modules would be more effective. This can be seen in

Table 5.3
Peaking Factor Comparison for Different Control Shell Locations.

Flush with Module			
Module #	Module	Radial	Axial
1	1.460978 ± 0.002607	1.536552 ± 0.159747	2.478462 ± 0.203752
2	1.532704 ± 0.002644	1.561906 ± 0.137605	2.474501 ± 0.199777
3	1.549082 ± 0.002664	1.549093 ± 0.129104	2.473575 ± 0.197486
4	1.567308 ± 0.002582	1.538523 ± 0.154474	2.655786 ± 0.199983
5	1.612465 ± 0.002712	1.551435 ± 0.126499	2.476989 ± 0.193737
6	1.580440 ± 0.002674	1.568756 ± 0.135958	2.473578 ± 0.196830
7	1.566631 ± 0.002676	1.562890 ± 0.156735	2.493255 ± 0.199095
4 cm Away From Module			
Module #	Module	Radial	Axial
1	1.585718 ± 0.002797	1.537947 ± 0.156635	2.205598 ± 0.180587
2	1.516406 ± 0.002715	1.536884 ± 0.138294	2.207890 ± 0.183556
3	1.577630 ± 0.002764	1.547760 ± 0.137572	2.217110 ± 0.181499
4	1.630888 ± 0.002715	1.540079 ± 0.155663	2.290358 ± 0.176278
5	1.467962 ± 0.002673	1.533203 ± 0.140435	2.236165 ± 0.188314
6	1.525078 ± 0.002729	1.533305 ± 0.137883	2.209708 ± 0.183162
7	1.446958 ± 0.002679	1.520046 ± 0.138348	2.212156 ± 0.187834

Fig. 5.6. Since during operations, all the shells would be utilized, optimizations of control shell properties should be conducted when all shells are inserted.

The placement of the shells were chosen to be further out at 4 cm from the module walls rather than being flush with it.

5.7.4 Control Shell Effectiveness

A shutdown margin of about 0.5$ with the central module stuck out is used in many reactors. The shutdown margin requirement ensures that the reactor can undergo a SCRAM even if the highest worth control element is stuck in the out position. To simulate this, the 6 outer control shells are placed at 100% insertion and the central shell is stuck out. Control shells of 2 cm thickness and located 4 cm away from the modules were used. This configuration gave a keff of 1.01591 $\pm$ 0.00102, which would still have the fresh core supercritical by almost 2.5$, i.e., this does not meet the shutdown margin requirement. Fission products after 3 days of operations add in about 1$ of negative reactivity, so the shutdown margin is still not achieved. A feasible configuration that had a shut down margin of 0.5$ could not be found. However, the control shells should never be 100% withdrawn so the shutdown margin maybe implemented differently such as physically not allowing the central shell to be withdrawn to a certain % such that the shutdown margin is achieved.

Using 2 cm control shells placed 4 cm away from the modules, a critical configuration (1.0001 $\pm$ 0.0001) was found with the side module shells at 75.5% inserted and the central shell 80% inserted. During operations, the shells would have to move to account for burnup of the core and fission product formation.

This analysis has shown control shells are a feasible method of controlling the reactor. In addition to these large shells, it maybe advantageous to have lower worth rods within the graphite matrix to act as regulating rods for fine control of the system. The addition of burnable absorbers within the modules can also help control the reactor.

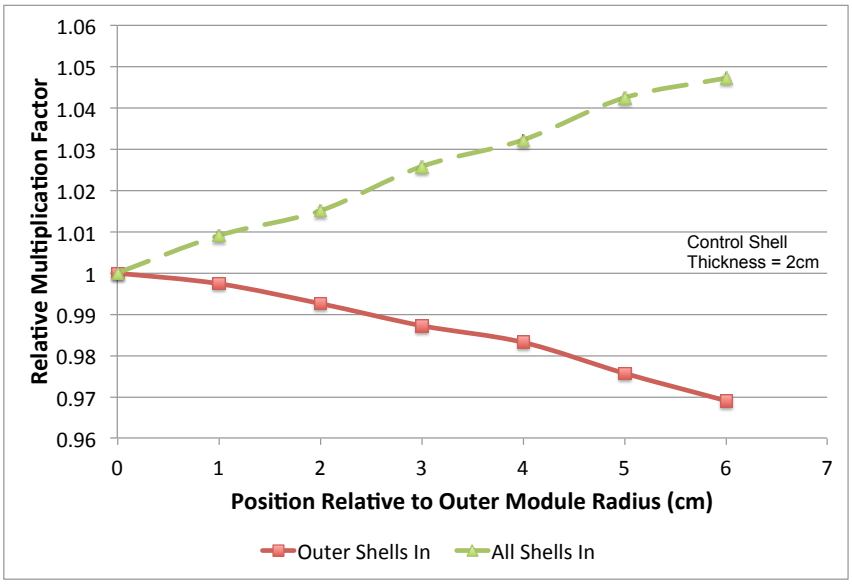

Fig. 5.6. Control Shell Position Effects.

6. CONCLUSIONS AND FUTURE DEVELOPMENTS

6.1 Future Work

A design basis for the HT-IMMTR has been created, though there is much work to be completed. This design should be the basis for future reactor analysis studies that includes a thermal hydraulics, balance of plant, and economics study.

The even burnup of the core through a flat power profile is very important, since this directly effects the core lifetime and economics. The inclusion of a central hole in the fuel region of each module would remove the fuel elements where the power typically peaks, and move the power peaks closer to the module periphery. The hole would also change the power distribution shape and can potentially flatten the profile, allowing a more even burnup of the core. Another method of controlling the power profile is to implement enrichment zoning. The periphery of the core can have higher enriched fuel than the center. This would increase the power density on the outer rim of the module and lower the density towards the middle, creating a flatter power shape. The inclusion of burnable absorbers throughout a module can decrease the initial reactivity worth of the modules as well as help shape the power profile.

The control of the core should be further developed. The inclusion of burnable absorbers within each module lowers the total reactivity worth of the core. This means the negative worth of the control elements can be lowered so thinner control shells can be used. Another means to control the core is the use of many control pins spaced throughout the graphite matrix between modules. If found viable, this scheme would allow for finer control of the reactor.

The use of BeO-UO_2 fuel versus UO_2 fuel on core lifetime has been investigated. The BeO-UO_2 fuel should also be compared with other fuels such as UC or TRISO in fuel compacts to assess the differences in core lifetime, safety factors such as power peaking and reactivity coefficients, and BOP characteristics. The use of a more

developed and tested fuel can allow for the HT-IMMTR to be built on a shorter time scale.

The economics of the reactor is an important aspect that needs further analysis, since an uneconomical plant will not ever be considered for commercial development. The fuel cycle costs with reprocessing should be investigated. Inclusion of BeO in the fuel adds an expense that needs to be accommodated by having a core with a large burnup, or reprocessing the fuel for BeO. The materials cost of the reactor should be estimated, and a construction plan that includes a cost analysis should be developed.

A thermal hydraulics analysis of the core must be developed. This analysis should detail the fuel, coolant, and moderator temperature distributions. These temperature distributions can then be used to update temperature dependent cross sections in the neutronics analysis to create a more accurate depiction of the core neutronics. The $ScCO_2$ natural convection capabilities to cool the decay heat of the core should be shown to demonstrate core safety during a SCRAM.

The balance of plant of the plant also needs more consideration. The $ScCO_2$ Brayton cycle machinery placement needs to be found and the cycle efficiency should be computed. Process heat generation machinery for use in the modules also needs investigation. The effects on the BOP on neutronics should also be analyzed and a control scheme for the reactor generated.

The licensing of the reactor under current guidelines, and the changes in guidelines needed to license the plant need investigation. The reactor is envisioned to operate near industrial sectors for process heat applications, or in rural locations under autonomous operation. These operating regions are not allowed under current NRC laws, so a change in licensing methodology would be required.

6.2 Conclusions

The High Temperature Integrated Multi-Modular Thermal Reactor is an SMR design that consists of several subcritical modules that are arranged in a single critical core configuration. Each module is self consistent in that it contains all the machinery needed for safe operations, except for the critical geometry. This configuration eliminates criticality accidents during construction and shipping, as well as allows for electricity generation or heat production concurrently since each module can have different BOP machinery.

A critical core with 7 subcritical modules arranged hexagonally in a critical configuration was designed in Serpent. Several fuel enrichments and BeO wt%'s were considered and a BeO-UO_2 fuel with 5 wt% ^{235}U and 5 wt% BeO was found to achieve a 14.6 year lifetime at 10 MW_{th}. Zirconium was found to be a better structural material than stainless-steel 304 due to Zirconium's neutronic properties.

Techniques on extending the core lifetime through battery type reshuffling and refueling were also analyzed. Module reshuffling during operations was found to not increase the core lifetime due to the relatively even burnup of the core, though more burnable regions should be used to verify this result. A batch style fuel reloading scheme was found to increase the core lifetime about half a year.

The use of several subcritical modules over one large core with one module was shown to be beneficial since a single module configuration would not be subcritical, and would be be very large compared to the subcritical module design. A single large module would remove many of the positive features of the HT-IMMTR.

The core flux and power distributions were found and power peaking factors calculated. Negative temperature coefficients of reactivity for the fuel, moderator, and coolant were found which allow for safe operations in the event of a transient. These distributions and factors can be used in future thermal hydraulics codes to further analyze the reactor.

The modules of the critical configuration were found to be subcritical at room temperature, which means criticality accidents could not occur during module construction. Two shipping accidents where water surrounded the module and where water entered the core were considered, and both left the modules subcritical. A LOCA event was considered and a negative reactivity insertion from the voiding of the $ScCO_2$ was found.

Control rods placed in several locations with various sizes were considered. Six control pins were found to not be able to create a critical core so cylindrical control shells were placed around each module. A critical configuration was demonstrated, though more control analysis needs to be completed.

In conclusion, a critical configuration of the HT-IMMTR was developed and analyzed, and design basis for future works has been created.

REFERENCES

Andrade, A., Alberto, R., Ferreira, N., 2007. Uranium dioxide and beryllium oxide enhanced thermal conductivity nuclear fuel development. In: International Nuclear Atlantic Conference. Santos, SP, Brazil.

Burnham, J. B., Merker, L. G., Deonigi, D. E., 1970. Comparative costs of oxide fuel elements. Tech. Rep. BNWL-273, Battelle-Northwest.

Carelli, M., 2009. The exciting journey of designing an advanced reactor. Nucl. Eng. Des. 239 (5), 880 – 887.

Chopra, O. K., Alexandreanu, B., Gruber, E. E., Daum, R. S., Shack, W. J., 2006. Crack growth rates of irradiated austenitic stainless steel weld heat affected zone in bwr environments. Tech. Rep. NUREG/CR-6891, ANL-04/20, Argonne National Laboratory, Argonne, IL, USA.

Dostal, V., 2004. A supercritical carbon dioxide cycle for next generation nuclear reactors. Ph.D. thesis, Massachusetts Institute of Technology, Cambridge, Massachusetts, U.S.

Gibbs, P., 2008. Power conversion system design for supercritical carbon dioxide cooled indirect cycle nuclear reactors. Master's thesis, Massachusetts Institute of Technology, Cambridge, Massachusetts, U.S.

IAEA, 2004. Innovative small and medium sized reactors: Design features, safety approaches and r&d trends. Tech. Rep. IAEA-TECDOC-1451, International Atomic Energy Agency, Vienna, Austria.

IEA, 2009. World energy outlook. Tech. rep., Organisation for Economic Co-operation and Development/International Energy Agency, Paris, France.

Ingersoll, D. T., 2009. Deliberately small reactors and the second nuclear era. Prog. Nucl. Energy 51 (4-5), 589–603.

Kim, S. K., Ko, W. I., Kim, H. D., Chung, Y., Bang, S., et al., 2010. Economic viability to beo-uo_2 fuel burnup extension. Nucl. Eng. Tech. 43 (2), 141–148.

Leppänen, J., 2010. Performance of woodcock delta-tracking in lattice physics applications using the serpent monte carlo reactor physics burnup calculation code. Ann. Nucl. Energy 37 (5), 715 – 722.

Leppänen, J., September 2011. PSG2 / Serpent – A Continuous-Energy Monte Carlo Reactor Physics Burnup Calculation Code. VTT Technical Research Centre of Finland.

MATLAB, 2010. Version 7.11.0 (R2010a). The MathWorks Inc., Natick, Massachusetts.

McDeavitt, S., Naramore, M., Ragusa, J., Revankar, S., Solomon, A., et al., 2010. Evaluation of high thermal conductivity oxide nuclear fuel concept containing beryllium. In: Proc. 2010 LWR Fuel Performance/TopFuel. Orlando, Florida, USA, Paper 138.

MEPS Online Steel Prices, 2012. <http://www.worldsteelprices.com/> (accessed 15.1.12).

Pelowitz, D (Ed.), April 2008. MCNPX User's Manual, Version 2.6.0. Los Alamos National Laboratory.

Shropshire, D. E., 2004. Lessons learned from gen i carbon dioxide cooled reactors. In: ASME Conference Proceedings. No. 46873. ASME, Arlington, Virginia, USA, pp. 463–473, 10.1115/ICONE12-49380.

Terai, T., Takahashi, Y., Masumura, S., Yoneoka, T., 1997. Heat capacity and phase transition of zircaloy-4. J. Nucl. Mater. 247, 222 – 226.

Ueki, T., Brown, F., November 2002. Stationarity diagnostics using shannon entropy in monte carlo criticality calculations i: f test. Trans. Am. Nucl. Soc 87 (156).

Wright, S., Radel, R. M., Rochau, V. G., Pickard, P., 2010. Operation and analysis of a supercritical co_2 brayton cycle. Tech. Rep. SAND2010-0171, Sandia National Laboratories, Albuquerque, NM, USA.

X-5 Monte Carlo Team, February 2008. MCNP — A General Monte Carlo N-Particle Transport Code, Version 5 Volume I: Overview and Theory. Los Alamos National Laboratory.

APPENDIX A
REACTOR CHARACTERISTICS

Table A.1: Reactor Characteristics

Properties	Value	Notes
Fuel	5%BeO-95%UO_2	wt%
Enrichment	5% ^{235}U	
Initial Fuel Loading	3384 kg	
Active Fuel Radius	.5 cm	
Cladding Thickness	2 cm	
Active Fuel Height	400 cm	
Number of Fuel Pins/Module	163	
Number of Modules	7	
Total Number of Pins	1141	
Fuel Pitch	10.5	$\frac{\text{pitch}}{\text{fuel diameter}}$
Module Pitch	1.1	$\frac{\text{module pitch}}{\text{module diameter}}$
Power	10 MW_{th}	Adjustable
Lifetime	14.6 years	
Coolant	Supercritical CO_2	
Clad, Vessel, Reflector	Zirconium	
Lattice Type	Hexagonal	
Module Diameter	161 cm	
Inner Pressure Vessel thickness	4 cm	

Continued on next page

Table A.1: Continued.

Properties	Value	Notes
Outer Pressure Vessel thickness	2 cm	
$ScCO_2$ Downcomer Thickness	400 cm	Should be determined by BOP
Upper plenum height	80.5 cm	Should be determined by BOP
Core Diameter	740 cm	Optimized = 640 cm
Outer Reflector Thickness	100 cm	Optimized = 50 cm
Upper and Lower Reflector Thickness	100 cm	
Control Shell Thickness	2 cm	
Control Shell Location	4 cm	Relative to outer module
β	0.00665	Delayed Neutron Fraction
Λ	1.17E-03 s	Mean Generation Time
l	1.42E-03 s	Prompt (Total) Neutron Lifetime

VITA

Name: Vishal K. Patel

Address: Department of Nuclear Engineering
Texas A&M University
337 Zachry Engineering Center, 3133 TAMU
College Station, TX 77843-3133

Email: VKP93@TAMU.EDU

Education: B.S., Physics, University of Texas at Austin, 2010
M.S., Nuclear Engineering, Texas A&M University, 2012